NTNU

Norwegian University of
Science and Technology

Mapping of demersal fish and benthos by Autonomous Underwater Vehicle equipped with optical and acoustic imagers at 600 meters depth in Trondheimsfjorden

Sverre Julian H Håpnes

Marine Coastal Development
Submission date: December 2015
Supervisor: Geir Johnsen, IBI
Co-supervisor: Martin Ludvigsen, IMT
Petter Lågstad, Forsvarets forskningsinstitutt

Norwegian University of Science and Technology
Department of Biology

Contents

Acknowledgements

The work of this thesis was carried out at Trondheim Biological Station (TBS), Department of Biology, NTNU, between August 2014 and December 2015.

First and foremost, I would like to thank my supervisor Geir Johnsen for giving me the opportunity to work with innovative technology in relation to biology. Your knowledge, infectious enthusiasm and boost made me believe in myself and in the importance of this work.

To my co – supervisors: Martin Ludvigsen and Petter Lågstad. Thanks, Petter, for compiling mosaics giving me the best possible starting point and Martin, for all the technical input and advice during the work of this thesis, it is truly appreciated.

In addition, I want to thank Christian Malmquist for giving timesaving advice when working in ArcMap and Øyvind Ødegård for giving my first lection in using Reflection.

To my fellow students and employees at TBS, for all the support, the pleasant conversations and social gatherings. You are truly lovely.

Thanks to family and friends for supporting me.

Sverre Julian Helmersen Håpnes, December 2015

Abbreviations

AUR-Lab	Applied Underwater Robotics Laboratory
AUV	Autonomous Underwater Vehicle
FFI	Norwegian Defence Research Establishment
HISAS	High Interferometric Synthetic Aperture Sonar
NGU	Norwegian Geological Survey
NTNU	Norwegian University of Science and Technology
OOI	Object(s) Of Interest
ROV	Remotely Operated Vehicle
SAS	Synthetic Aperture Sonar

Abstract

The marine environment is largely under-sampled both in time and space. There is a growing need for more automated approaches to provide a better understanding, identification, mapping and monitoring of biogeochemical processes for future environmental management of biological resources present in or around the seafloor.

This thesis aims at identifying and mapping demersal fish and benthos by means of an autonomous underwater vehicle (AUV) for establishing non-invasive measurements on abundance of fish and benthos. Future prospects include implementing these findings for future nature management and decision-making.

A soft bottom community compiling demersal fish and benthos in the Agdenes deep water basin was surveyed using the HUGIN HUS AUV at a depth of approximately 600 m. Imagery provided by a photomosaic camera (high spatial resolution) and a synthetic aperture sonar (high spatial coverage) covering 39 200 m^2 of seafloor were used for identification and mapping biological objects of interest (OOI).

The findings indicates relatively high abundance of Herring smelts (Argentinidae spp.) and Rabbit fish (*Chimaera monstrosa*) and a wide spread distribution of other demersal fish species. Benthos, including sea stars, anemones and crabs, were relatively numerous.

The sonar provided imagery of high spatial coverage, but the spatial resolution was considered to be too low for detection of biological OOI under present conditions. The photomosaic camera provided imagery of high spatial resolution enabling identification of fish species and other benthos to family or order. The AUV is considered to be a suitable tool for mapping biological habitats, being an efficient and adaptable platform for surveying features of biological significance.

Sammendrag

Det marine miljøet er lite undersøkt både i tid og rom. Det er en voksende interesse for mer automatiserte metoder for å gi en bedre forståelse, identifisering, kartlegging og overvåkning av biogeokjemiske prosesser for fremtidig forvaltning av biologiske ressurser på havbunnen.

Denne oppgaven tar for seg identifisering og kartlegging av bunnfisk og bentos gjennom bruk av en autonom undervannsfarkost (AUV) for dannelse av ikke-invasive mål på tallrikhet av fisk og bentiske organismer. Dette gjøres med tanke på fremtidig naturforvaltning og beslutningstaking.

Et bløtbunnssamfunn av bunnfisk og bentos i dypvannsbassenger i Agdenes ble kartlagt ved bruk av HUGIN HUS AUV ved 600 m dyp. Bilder fra fotomosaikkamera (høy romlig oppløsning) og en syntetisk apertur sonar (høy romlig dekning) av 39 000 m^2 havbunn ble brukt for identifisering og kartlegging av biologiske objekter av interesse (OOI).

Funnene indikerer relativt høy tallrikhet av Argentinidae spp. og *Chimaera monstrosa* og en bred fordeling av andre bunnfisk. Andre bentos, inkludert sjøstjerner, anemoner og krabber, var tallrike.

Sonaren produserte bilder med høy romlig dekning, men den romlige oppløsningen ble vurdert å være for lav for å detektere biologiske OOI under gitte betingelser. Fotomosaikkameraet produserte bilder med høy romlig oppløsning som åpnet for identifisering av fisk til art og andre bentos til familie eller orden. Den autonome undervannsfarkosten er ansett for å være et egnet verktøy for kartlegging av biologiske habitater på grunn av dens effektivitet og tilpasningsdyktighet.

1 Introduction

The marine environment is under constant pressure due to anthropogenic influence as we increase our dependence on it (Goldberg (1995), Halpern et al. (2008)). There is a growing need for a better understanding of marine habitats in general. To provide more automated approaches to understand, identify, map and monitor marine organisms we need new enabling technology to achieve this. The marine (and aquatic) environment is largely under-sampled both in time and space (Dickey et al., 2008). Few methods are developed to provide information of taxa, distribution and biomass of marine organisms associated with seafloor (benthic zone). The long and complex Norwegian coastline, comprising fjords and 71 963 islands (Statistics Norway, 2013), makes detailed field-mapping difficult for both practical and economical reasons (Bekkby, 2009). There is, however, a growing interest in mapping of benthic communities, as more stakeholders are interested in utilizing the resources found in or around the seabed (e.g. the MAREANO project, Buhl-Mortensen et al. (2010), Harris and Baker (2012)). Mapping of benthic habitats is believed to be crucial in terms of allowing scientist and environmental managers to grasp the distribution of biotic and abiotic constituents on the seafloor (Shumchenia and King, 2010). As estimates of demersal fish (those living in association with the seafloor) abundance are of limited benefit provided by fishery due to restrictive catch limits, there is a need for more automated non-invasive approaches (Ferrini and Singh (2006), Clarke et al. (2009)). The use and constant development of underwater vehicles as instrument carriers for sea exploration provides a large variety of new applications for biogeochemical research and nature management (Moline et al. (2005), Johnsen et al. (2013), Ludvigsen et al. (2014)). The driving force for this development have been the defence and the petroleum industry, whereas the scientific community has later on applied the new instrument carrying platforms. Marine biology as a field has in recent times seen a paradigm shift from off-line sampling to continuous monitoring throughout utilizing this enabling technology (Delaney et al. (2001), Clarke et al. (2009), Berge et al. (2012), Ludvigsen et al. (2014), Berge et al. (2015)).

Autonomous underwater vehicles (AUVs) are untethered, pre-programmed and self-propelled robotic vehicles that can be supported with a range of different instruments for mapping and monitoring features of interest (von Alt (2003), Singh et al. (2004)).

Two instruments mounted on a HUGIN 1000 AUV (see Material and Methods) were used to collect data processed in this thesis. To cover larger areas, a high interferometric synthetic aperture sonar (HISAS), was used to obtain images from acoustic signals of the seafloor with high resolution (<5x5 cm) and a spatial coverage of up to 260 m on each side of the vehicle (Fossum et al. (2008), Hagen et al. (2008a)). To provide data with a higher spatial resolution than HISAS and with a lower area coverage, a monochromatic photomosaic (collection of images merged to form a large image) camera was used. Optical images of the seafloor were obtained with an observed spatial resolution of approximately 1x1 cm (Figure 20 and 21) at a frequency of 2 Hz.

The aim of this thesis is to create maps based on two sensors: a monochromatic photomosaic camera and HISAS for biological information, to obtain larger spatial coverage and to estimate the density of demersal fish and benthos (species that live on, in or near the benthic zone, hence termed benthos or benthic organisms). Further, the sensors are evaluated according to the following criteria: 1) as tools to identify, map and monitor different species of demersal fish and benthic organisms, 2) as tools for future nature management and decision making. Quality requirements for still image and/or video surveys listed in European standard (European Committee for standardization, 2012) are discussed with respect to own observations.

2 Theory

2.1 Habitat description

Trondheimsfjorden is the third longest fjord in Norway (Statistics Norway, 2013) and consists in general of hard bottom in the steep regions and soft bottom with sludge, mud and clay in the deep basins (Sakshaug and Sneli, 2000a). Another characteristic is the large amount of river water supplying the fjord with particles, nutrients and metals (Sakshaug and Sneli, 2000b). The study area is within the outermost, deepest region of the fjord consisting of soft bottom. The biodiversity of the soft bottom fauna is affected by environmental factors, such as current speed and direction, together with temperature, pressure and salinity. Most of the animals live in the sediments (Sakshaug and Sneli, 2000c), but the dumping of anthropogenic structures supplies the relative homogenous soft bottom with hard structures enables the creation of new habitats (Zintzen et al., 2008). Studies done on debris (Watters et al., 2010) and ship wrecks (Zintzen et al., 2006) have revealed that anthropogenic structures might suite as artificial attachment sites and seafloor habitats for some groups of species (Ludvigsen et al., 2015). The area of interest has a history with dumping of ammunition and condemned vessels (Sakshaug and Sneli, 2000a) and the dumping of military surplus after World War II (WWII) has been granted a lot of attention the latest years (e.g. Ludvigsen et al., 2015).

2.2 Platform and sensors

An AUV was used in this project, a self-propelled autonomous underwater vehicle pre-programmed to follow a designated route over the sea floor. Mounted on the AUV a sonar system and a photomosaic camera were used to produce images of the sea floor with different spatial resolution of images and corresponding areal coverage (See Table 1 and 2 for more information).

2.2.1 Autonomous underwater vehicles

The earliest AUV technology dates back to the development of the Self-Propelled Underwater Research Vessel (SPURV) in the beginning of the 1960s at the University of Washington (cited in Moline et al., 2005). Constant technological development expanded the possibilities of AUVs as instrument carrying platforms (Gafurov and Klochkov, 2015). Integration of this technology opened for multiple applications including educational, scientific, military and especially for environmental research, see Moline et al. (2005).

AUVs are unmanned vehicles that propagate through the water masses by a propulsion system, while controlled in three dimensions by on-board systems for guidance, navigation and control. This allows the vehicle to accurately follow pre-programmed trajectories relatively independent of environmental variables (von Alt, 2003). AUVs can be divided in two main classes: gliders and propeller-driven AUVs. Autonomous gliders use the change in buoyancy over their wings to convert a part of the vertical motion to horizontal velocity, enabling long-term subsurface missions ranging from weeks to months, with low energy demand and corresponding payload capacity. Propeller-driven AUVs facilitate a higher payload capacity enabling multiple instruments to work in concert, where battery capacity and depth rating are the main limiting factors (Moline et al., 2005).

Sensors mounted on the AUV map the surrounding environment as the vehicle propagates through the water masses enabling both spatial and time series measurements. Collected data is automatically geospatially tagged and temporally referenced (von Alt, 2003). This separate AUVs from other platforms like moorings and autonomous profilers, which are limited to a specific location and satellites and airborne sensors, which are typically limited to measurements in the surface (Moline et al., 2005).

A propeller-driven AUV, HUGIN 1000 (denoted HUGIN or HUGIN AUV) featured in Figure 1, was the instrument-carrying platform used to obtain data used in this project (see details in Table 1).

Figure 1. HUGIN 1000 AUV with HISAS (HISAS 1030, two on each side of vehicle) (Geomares Publishing bv, 2012 - 2015).

2.2.2 HUGIN AUVs

The HUGIN AUVs are a result of a collaboration program between Kongsberg Maritime and the Norwegian Defence Research Establishment (FFI) and features different instrument configurations and depth ratings. The HUGIN AUV program started out in the beginning of the 1990s with a civilian and military approach (see Kongsberg Maritime (2009) for more information). Data from a survey conducted with *Hugin HUS*[1], a HUGIN 1000 AUV (currently the smallest AUV in the HUGIN family), was used in this project. The vehicle has a depth rating of 3 000 m and speed range of 2-6 knots allowing operational endurance of 18-24 hours. The high payload capacity enables the mounting of a wide variety of instruments facilitating different approaches targeting military and oil industry, as well as civilian scientific and commercial tasks (Hagen et al. (2003), Kongsberg Maritime (2009)).

[1] Operated and maintained by a Norwegian national collaboration led by FFI

Table 1. Key specifications of the HUGIN 1000 AUV (Adapted from Kongsberg Maritime (2009)). Abbreviations denote: Multibeam Echo Sounder (MBE), Side Scan Sonar (SSS), Sub Bottom Profiler (SBP) and Conductivity Temperature Depth (CTD).

HUGIN 1000, basic specifications	
Dimensions	
Weight	650-840 kg
Length	4.7 m
Diameter	0.75 m
Depth rating	3000 m
Dynamics	
Speed	2-6 knots
Battery	
Capacity	15 KWh
Endurance	24 hours at 4 knots (with MBE, SSS, SBP and CTD)

2.2.3 HISAS 1030

The HISAS 1030 is a complex interferometric synthetic aperture sonar (SAS) system developed by Kongsberg Maritime. The basis of SAS is to combine several pings overlapping an area, due to the synthesis of a long antenna in the azimuth (along-track) direction, to increase corresponding resolution (Figure 2). HISAS 1030 provides acoustic images of high resolution at long ranges (range independent) with co-registered bathymetry (See table 2 for more information) by replacing sonar-hardware with computer-processed data. The system compiles two 1.2 m long arrays with a field of view of up to 30° on each side of the vehicle, illustrated in Figure 1 (See Fossum et al. (2008), Ludvigsen et al. (2014) for more information).

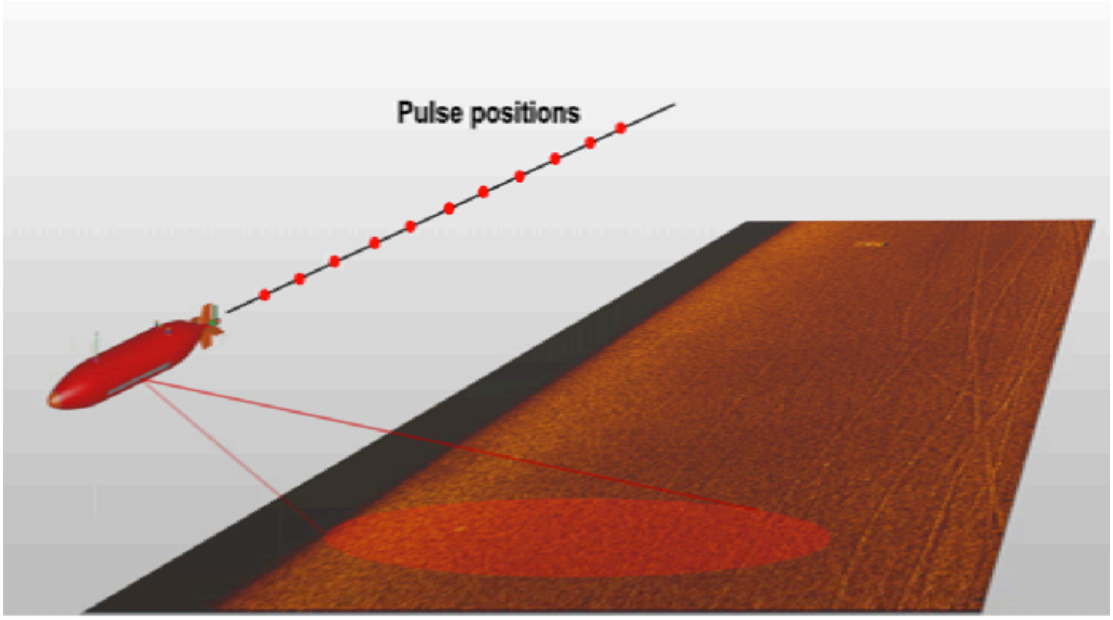

Figure 2. The principle of synthetic aperture sonar (Fossum et al., 2008).

Table 2. Comparison between HISAS (acoustic imagery) and photomosaic camera (optical imagery) (Fossum et al. (2008), Kongsberg Maritime (2009)). Some of the values are approximations as they are obtained from this survey.

Instrument	**Frequency**	**Maximum range (sides of the vehicle)**	**Theoretical spatial resolution (across-track x along track)**	**Observed spatial resolution**	**Operational altitude (approx., from this survey)**	**Coverage rate (km^2/hour)**
HISAS 1030	60-120 kHz	200 m at 4 knots)** 260 m at 3 knots)**	2x2 cm	> 5x5 cm	25-30 m	2.628 km^2/h (operation geometry dependent)
Camera (Illunis XMV-11000)	2 Hz	Altitude dependent	0.15x0.15 cm	1x1 cm*	6-6.5 m	0.0216 km^2/h

*Obtained from seafloor imagery of this study (software dependent).

** Dependent on speed of AUV

2.2.4 Tilefish camera system

Tilefish is a camera system designed for HUGIN with a sensitive camera (Illunis XMV-11000, Illunis LLC, USA) and large optics supported with strobed green LED (light emitting diodes) lights. The camera system captures black – and – white (monochromatic) images customized to distant imaging of green up – welling irradiance (E_u). Mounted on the HUGIN AUV (Figure 3), the Tilefish camera runs at 2 Hz image rate (2 images a second) providing detailed seafloor imagery with an operational altitude of approximately 6 – 6.5 m (See table 2 for additional information). To minimize the extent of backscatter, there is a 1 metre distance between camera and LED panel (Schjerven (2009), Ludvigsen et al. (2014)). Images are digitally compiled to form a photomosaic using designated software. For simplicity, the camera system is referred to as a Tilefish camera or photomosaic camera.

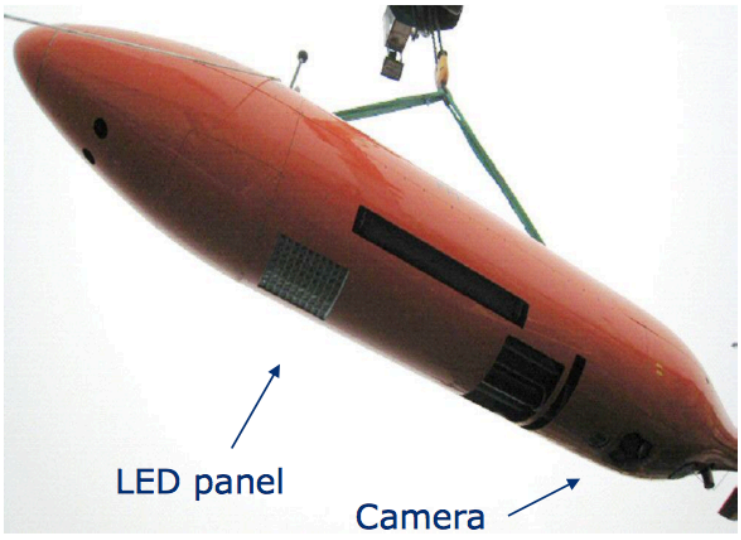

Figure 3. Hugin AUV illustrating the position of and spacing between the LED panel and camera (Schjerven, 2009).

2.3 Biological applications

Still image capture has been used for decades in the process of mapping the species composition and abundance of epibenthic megafauna, namely organisms large enough to be detected on a photograph (organisms >1 cm that live in the sediment-water transition zone) , e.g. Grassle et al. (1975), Smith Jr et al. (1993), Meyer et al. (2013). Two main strategies of optical mapping the megafauna exist including fixed-point measurements and transect measurements (Sherman and Smith Jr. (2009), Dolan et al. (2009), European Committee for standardization (2012)). Several efforts of optically imaging the seabed using still camera on an AUV have succeeded including the Seabed AUV photo mosaics (Singh et al. (2004), Ferrini and Singh (2006), Singh et al. (2007), Clarke et al. (2010)) and the *Sirius* AUV (a modified Seabed AUV) photo mosaics (Williams et al. (2009), Barrett et al. (2010)).

HISAS 1030 is a AUV mounted sonar system originally developed for military mine detection on the seafloor (Fossum et al., 2008), though the instrument can be used for multiple scientific applications including archaeology (e.g. Odegard et al., 2013) and geology (Denny et al., 2015). McHugh (2000) claimed that SAS technology had to be developed for applications within marine biology, though there exist, to my knowledge, only a few studies aiming at mapping seafloor for biological traits by means of a SAS (Ekehaug (2013), Ludvigsen et al. (2014), Ludvigsen et al. (2015)).

3 Material and Methods

The following section explains how and where the data were collected, which demersal fish species and benthos that are associated with the survey area and how the data were processed for analysis.

3.1 Data acquisition of area

The data from the HISAS and the Tilefish camera (generating monochromatic photo mosaics) were collected *in situ* in the Agdenes deep-water basin at 600 m depth in the outermost part of Trondheimsfjorden 9^{th}-13^{th} of December 2013 (coordinates

(decimal degrees) obtained as latitude and longitude enclosing the study area (Figure 5) were approximately: Upper left corner: 63.62 and 9.77, upper right corner: 63.62 and 9.78, lower left corner: 63.60 and 9.77, lower right corner: 63.60 and 9.80). The sampling of data used in this thesis occurred at the same location for two following days (10^{th}-11^{th}). This, as a part of a collaboration survey conducted by FFI, Norwegian Geological Survey (NGU), NTNUs Applied Underwater Robotics Laboratory (AUR-Lab) and Ecotone (Ecotone AS, Trondheim, Norway) to investigate and map possible effects of the dumping of military surplus such as bombs and mines from the end of WWII.

Figure 4. Map of Norway with the study area indicated with red dot (outlet of Trondheimsfjorden).

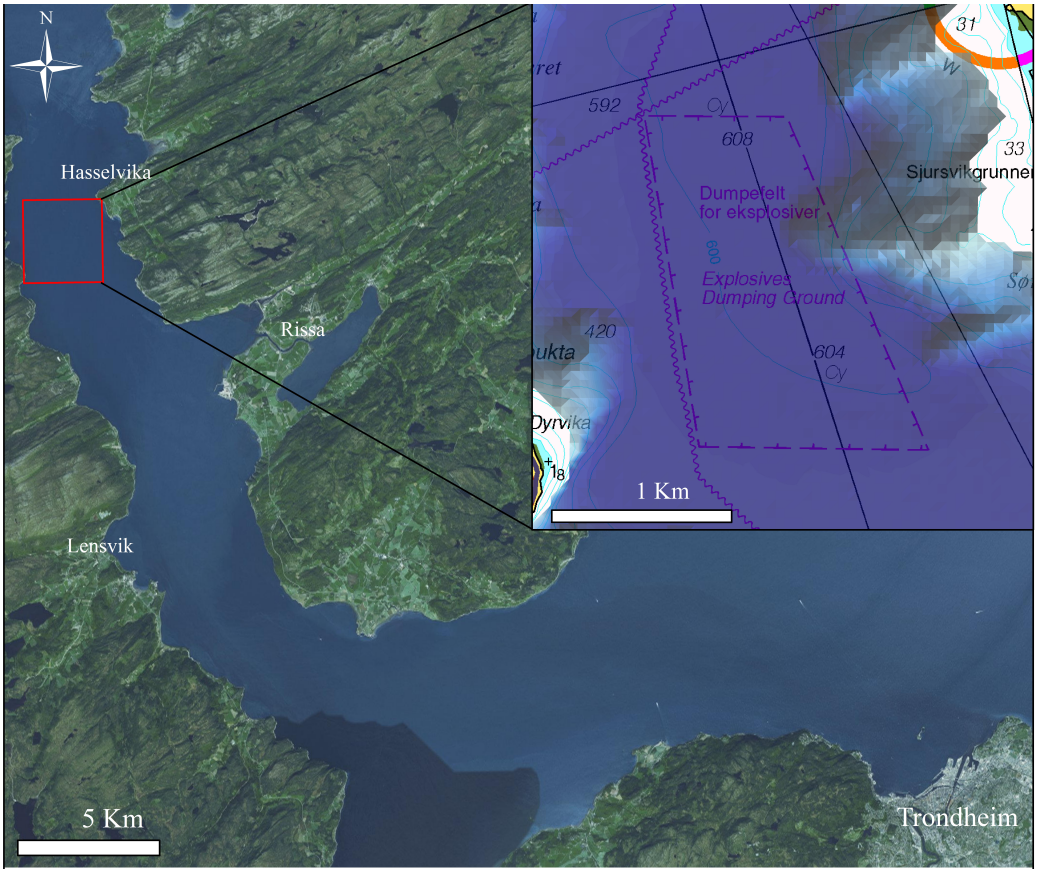

Figure 5. The study area is located in the outermost part of Trondheimsfjorden. The inset map shows the outline of the explosive dumping ground where the data for this study were collected.

A HUGIN 1000 AUV, owned and operated by the FFI, collected data where a HISAS and a monochromatic photomosaic camera were among the instruments carried by the AUV and constitute the data sources in this thesis. HISAS data were downloaded and processed by means of FFI´s *FOCUS* software, and the data from the monochromatic photomosaic camera were processed in Reflection (clipped and merged to form mosaics compiled in files of 1000 images by Petter Lågstad/FFI). The screening of the dumping field resulted in a coverage of approximately 2.1 square kilometre (2 100 000 m^2) by HISAS and 0.1 square kilometre by the monochromatic photomosaic camera (AUR-Lab and FFI, 2013).

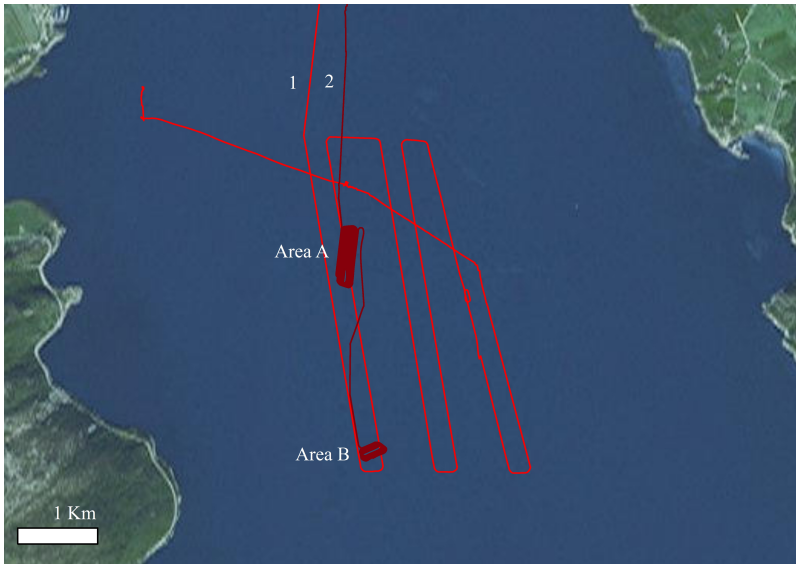

Figure 6. Navigation transects for the HUGIN 1000 AUV within the study area. Line 1 (bright red) and 2 (dark red with area A and B) denotes transects for HISAS and monochromatic photomosaic camera, respectively. Labels “Area A” and “Area B” indicates areas of interest surveyed with photomosaic camera.

3.2 Fish species associated with the survey area

The deep areas of Trondheimsfjorden hold a relative low biodiversity of benthic organisms, in terms of both species and individuals. However, the number of individuals can be as high as 1000 per m^2 at 500 m depth (Sakshaug and Sneli, 2000c). In this study, fish detection and mapping is the major focus. A brief description of the fish associated with the surveyed area is shown in Table 3.

Table 3. Brief description of some fish associated with the study area. For taxonomic description, see Muus and Nielsen (2012), Moen and Svensen (2004).

Family	Species	Habitat	Maximum length (cm)	Living depth (m)	Food source
Lotidae	Cusk (*Brosme brosme)*	Various bottom	90	70 -1 000	Crustaceans, molluscs, fish
Chimaeridae	Rabbit fish (*Chimaera monstrosa*)	Soft bottom	150	300-500	Molluscs, urchins, fish
Argentinidae (Herring smelts)	Greater argentine (*Argentina silus*)/	Bottom*	70	150-1 400	Crustaceans, octopus, fish
	Lesser argentine (*Argentina sphyraena*)	Soft bottom	30-35	50-500	Crustaceans, polychaetes, fish
Scyliorhinidae	Blackmouth catshark (*Galeus melastomus*)	Various bottom	90	150-200	Crustaceans, molluscs, fish
Myxinidae	Atlantic hagfish (*Myxine glutinosa*)	Soft bottom	80	20-600	Benthic organisms
Lophiidae	Angler (*Lophius piscatorius*)	Soft Bottom	200	-1 000	Fish, lobster, crabs, octopus
Macrouridae	Rock grenadier (*Coryphaenoides rupestris*)	Soft bottom	110	160-2 000	Shrimps, benthos
Pleuronectidae (Righteye flounders)	Witch flounder (*Glyptocephalus cynoglossus*)	Soft bottom	60	50-1 500	Polychaetes, crustaceans, bivalves, brittle stars

* Type of bottom not specified in literature.

3.3 Data processing

The data processing was as a whole done at TBS interpretation lab equipped with the designated software and hardware (detailed below).

3.3.1 Reflection

The software package "Reflection" (Version 2.1.2) developed by Kongsberg Maritime was used to process the images from the monochromatic photomosaic camera and sonar images from HISAS (see Figure 7 for workflow).

12 000 images from the monochromatic photomosaic camera were processed and analysed for biological object(s) of interest (OOI) associated with the seafloor with focus on demersal fish. Identification characteristics for OOI were established (exemplified in Figure 11-14). OOI were identified and entered in an Excel worksheet for data overview. Uncertain identifications were marked and gone through at the end of the period. Objects believed to be fish with an observed length of below 0.3 m were excluded due to lack of detail (too low spatial resolution). The sea anemones were classified based on if they appeared to be attached to hard or soft substrate and only individuals with visible tentacles were counted. The photomosaic dataset was initially processed throughout a limited period (12 days) to avoid the presence of bias related to knowledge level of user. This was followed by a longer systemizing period (30 days of verification and quality assessment) to cope with OOI with less distinguishable morphological characteristics.

Lowest threshold for species identification was specified for each taxa (lowest identifiable taxa level, see Table 4 in result section) to make the identification process as correct as possible. Sections of the data were cut out to prevent the extent of image overlaying present and then exported to ArcMap (Version 10.3, Esri, Redlands, US) as photomosaic sequences compiling 6 379 images covering an area of 39 200 m^2. Images of OOI were extracted from the dataset for positive identification and presented in the Results section.

HISAS data representing the same area (39 000 m^2) as the corresponding photomosaic sequences were screened for OOI, and further compared to the monochromatic photomosaic within the ArcMap software.

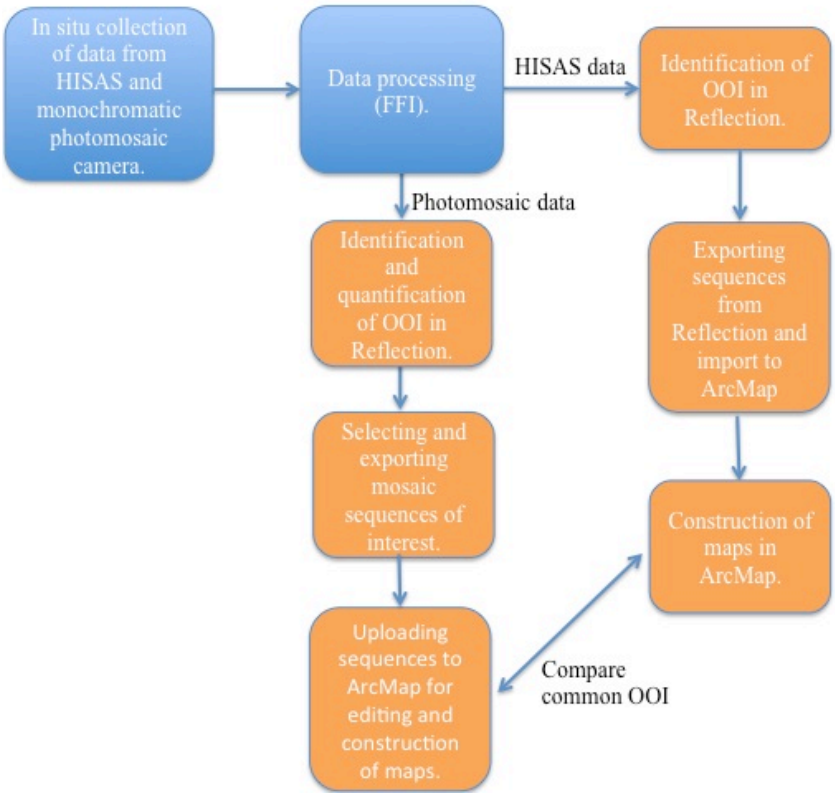

Figure 7. Overview of the workflow used in this project. The blue squares illustrate work done by FFI and/or Petter Lågstad, while the orange squares illustrate work done in this project.

3.3.2 ArcMap

ArcMap, a part of Esri's geographical information system (GIS) software suite, was used to create maps including metadata to place the survey sites in an easily interpretable context (due to the fact that each pixel in the data is geo-referenced). The selected data was imported to ArcMap to obtain a larger spatial coverage and allowed fragments of the data to be highlighted as well as comparing the data from the different instruments. Editing in ArcMap made merging of the mosaic data in a good way through colour optimization for a best possible presentation. This also opened for erasing existing noise in the corners (typically distorted and/or dark areas) of the original mosaic images, and made the transition between the different layers visible for the viewer.

4 Results

The following section describes the major findings in this thesis presented in a chronological matter. Figures and tables are presented to give an adequately detailed picture of the mapping of seafloor using HISAS and photomosaic camera, the spatial distribution of OOI, as well as a comparison of different processed images from the photomosaic camera. The surveys with the two different instruments were performed at different times, thus it did not allow direct image comparison of moving objects (fish). Because of the nature of data, I present the result with a focus on graphical information and compile the take home messages in the tables.

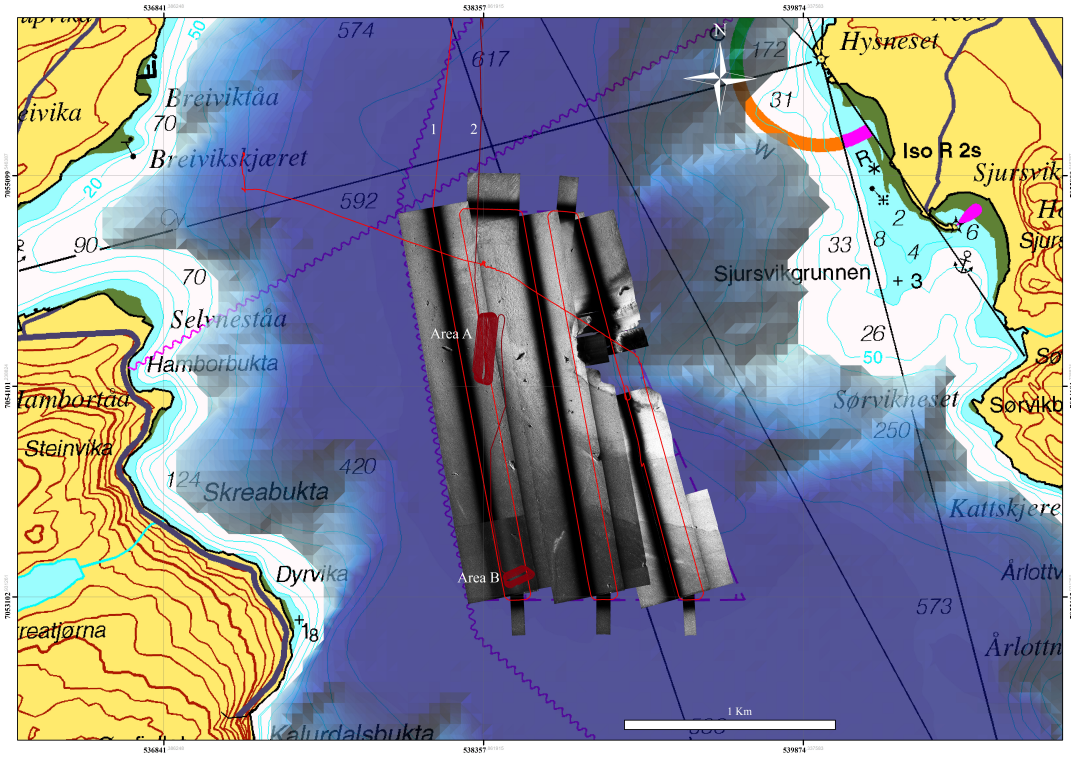

Figure 8. The study area covered with HISAS imagery and trajectories for collection of HISAS and monochromatic photomosaic camera data (indicated by bright and dark red lines) labelled 1 and 2, respectively.

4.1 HISAS imagery for detection of OOI and mapping of the seafloor

HISAS data covering the same area as the data from the photomosaic camera (approximately 39 200 m^2) were screened for biological OOI. This was done due to

the presence of interesting structures as patches of fish in the photomosaic sequences and the possibility to compare imagery from the two instruments. Figure 8 illustrates the spatial coverage of the HISAS providing an image and the survey area and lines for the two instruments (1 and 2). Objects that looked similar to fish were observed in the data, but the degree of uncertainty (related to spatial resolution) led to that it had to be omitted from the data presented.

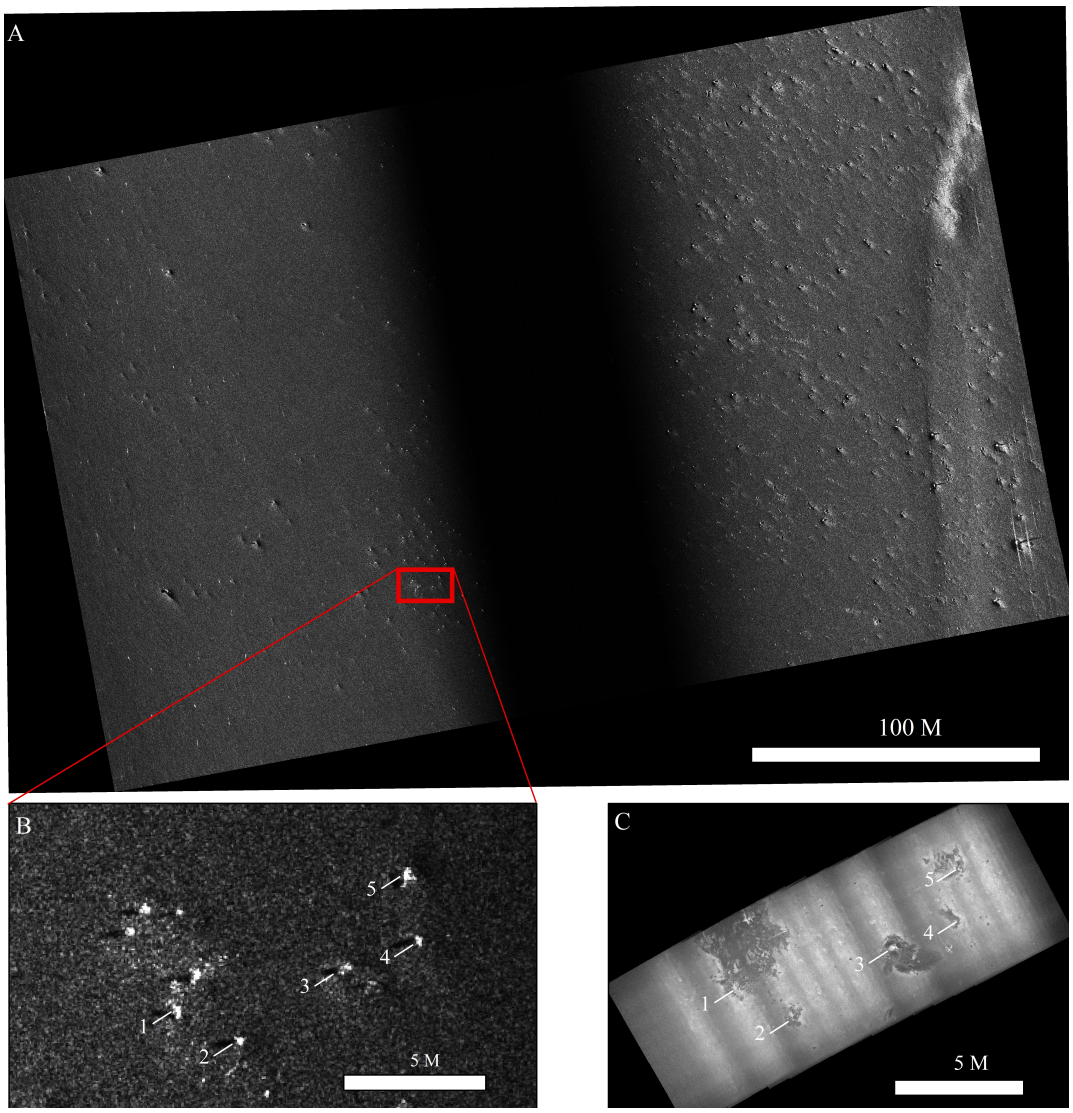

Figure 9. HISAS imagery from area B (A) with inset map (B) and corresponding photomosaic imagery. White signals indicate hard OOI seen by HISAS (B), which were found to be bombs in photomosaic image (C). Labels 1-5 in both images indicate bombs on the seafloor. Image B and C provides information on what can be seen on output from the different instruments. Each pixel is geo-referenced, thus enables comparison of similar structures (B and C). Note that the scale is different for A and B.

The presence of anthropogenic structures including military surplus was stated in advance of this project and objects believed to be of anthropogenic character was seen throughout the entire dataset. The different level of detail seen in Figure 9 (B and C) and 10 (A and B) exemplifies what can be obtained of information from the HISAS and photomosaic camera respectively.

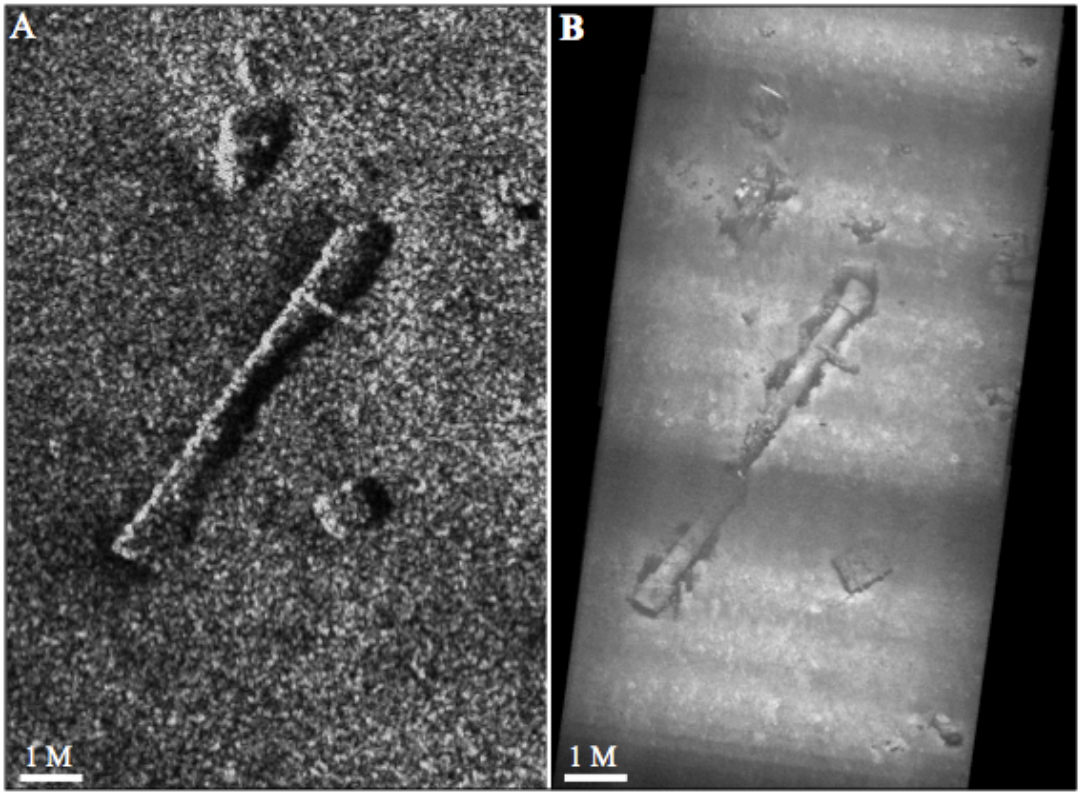

Figure 10. HISAS image (A) and photomosaic imagery (B) of pipe of unknown origin from area A illustrates the level of detail (spatial resolution) that can be obtained from the two instruments. Note that the scale is different for A and B.

Objects believed to be bombs (Figure 9) appear as bright white structures (Figure 9 B, labelled 1-5) and can be ground truthed through the detailed image in Figure 9 C. Figure 9 C provides a more detailed image (higher spatial resolution) in terms of the biology attached to and surrounding the bombs compared to Figure 9 B. Due to the geo-referencing of each pixel in both imaging techniques, the images (Figure 9 B and C) were shown to represent the same area.

Corresponding structures were also recognised in the data from the two instruments in area A. Figure 10 A shows the outline of a elongated object from an HISAS image, whereas Figure 10 B provides a more detailed image from photomosaic camera of what presumably is a cylindrical pipe in either metal or concrete due to the presence of pipe sockets.

4.2 Identification of OOI and mapping seafloor using monochromatic photomosaic camera

Approximately 12 000 still camera images were screened for the presence of biological OOI whereas 6 379 of them (approximately 39 200 m^2) were used for mapping and statistics in this thesis. The spatial resolution of the images allowed for some specimens to be identified to species, others to family or order, while numerous objects were excluded from the data handling due to lacking information in the images. Several factors including brightness and sharpness and of the images complicated the identification process (see Discussion).

Figures 12-15 represent mosaic imagery of some of the main fish species including schematic drawings form a bird's perspective used for ground truthing in the identification process. Specimens of Actiniaria (class Anthozoa that includes sea anemones) and Rabbit fish were the most numerous biological OOI observed in area A, whilst specimen of Herring smelts (aka Argentines) and Actiniaria were most numerous in area B.

The photomosaic images in Figure 11 illustrate the spatial distribution of the fish findings as well as a visual impression of the presence of the different fishes in the covered area. Due to overlaying of photomosaic sequences (different transect lines), a portion of the data had to be excluded. The per cent overlaying present in the results is 19.15 and 17.75 for area A and B, respectively (See table 4 for more information).

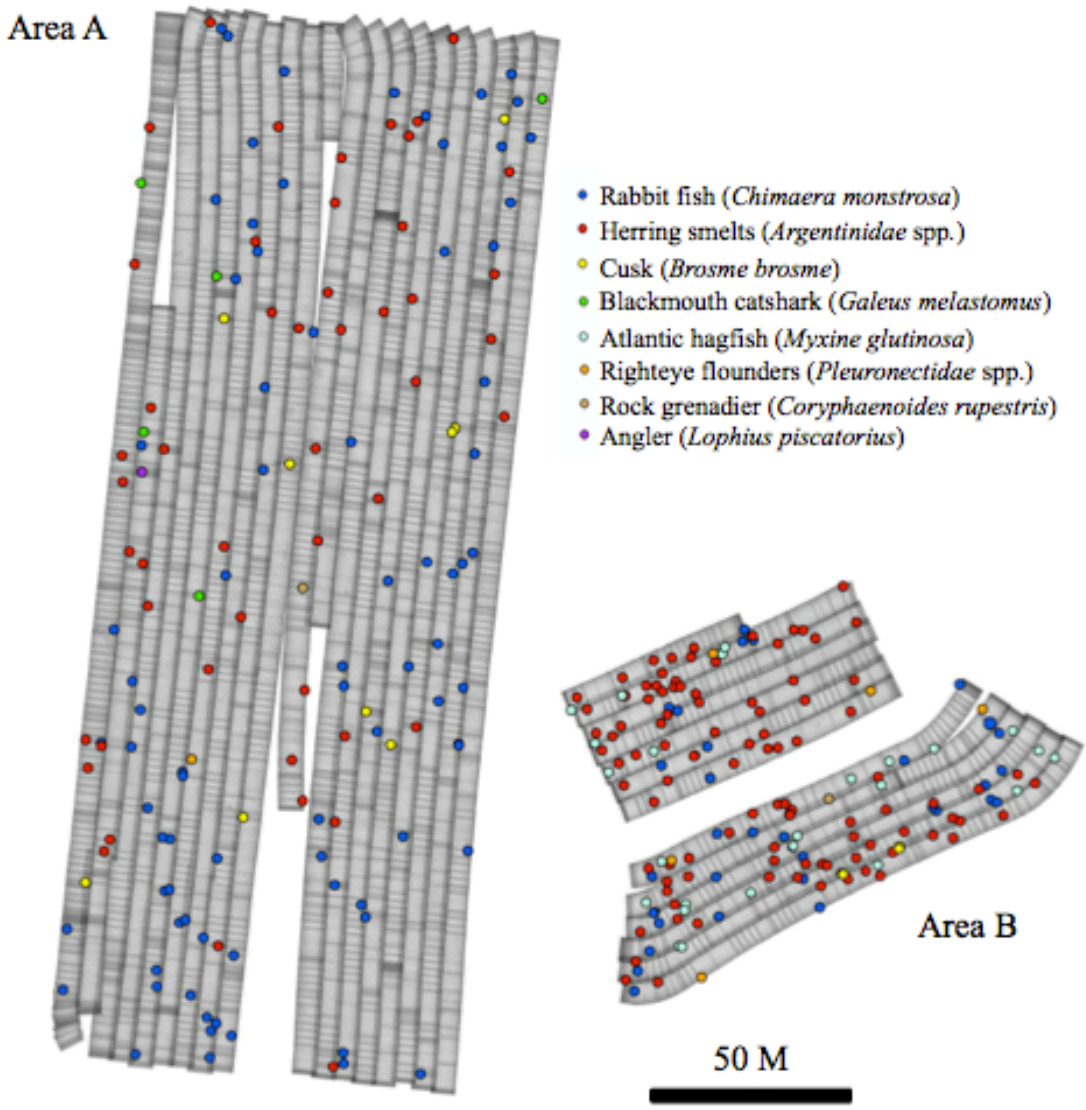

Figure 11. Overview of photomosaic of fish species and numbers in area A and B. Labels with colours representing the observations of the different species are placed in a spatial context. For species enumeration, see Table 4.

The number of fish counted in area B was higher (173 individuals) compared to area A (145 individuals) which is surprising taking into account that area A has approximately four times the area as area B. It should be mentioned that the Herring smelts and Atlantic hagfish represented the most numerous groups in area B, whilst the relationship between the two areas was relative even for the other fish numbers in relation to counted areas.

It should be mentioned that there was an observed difference in bottom structure between area A and B; where area A held a larger quantity of artificial structures compared to a more homogenous bottom structure in area B.

The lowest registered number of fish was seen for the Angler, Rock grenadier and Pleuronectidae (Righteye flounders) species for area A, and rock grenadier and Blackmouth catshark for area B. Species found in only one of area A and B were Angler and Atlantic hagfish, respectively.

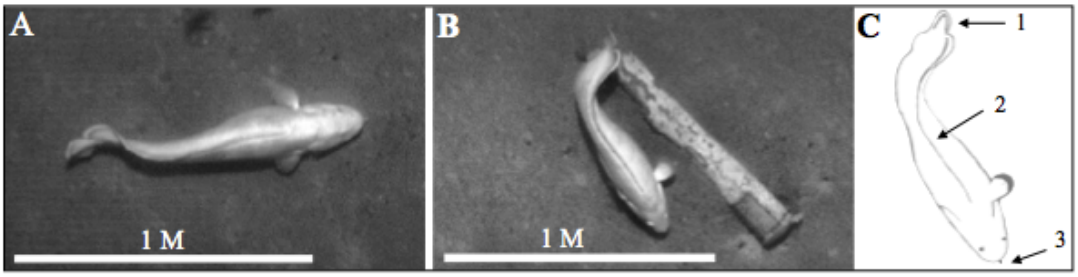

Figure 12. Pictures of Cusk (*Brosme brosme*) captured with monochromatic photomosaic camera (A and B). C displays a schematic drawing of species specific characteristics: In a "bird's-eye view", label 2 and 1 indicates one long dorsal fin with a white edge, barely connected with the round caudal fin, respectively. 3 indicates presence of a chin barbel (Muus and Nielsen, 2012).

4.3 Spatial distribution of demersal fish

Placing the fish findings in a spatial context provides potentially valuable information on the scope of fish represented within a certain area of soft bottom as well as a quantification of individuals occurring. Being the main focus, the fish findings are solely illustrated in a spatial context (Figure 11), additionally they represent the most numerous group identified to species (For abundance, see Table 5).

It emerges from Table 4 that the Herring smelts is the most numerous fish family in the dataset with spread distribution in area A and a more patchy distribution in area B (Figure 11). The Rabbit fish was the most numerous fish species recorded in area A, labelled dark blue in Figure 11, also with a wide distribution. The specimens of Cusk were observed spread throughout the dataset, primarily around or within solid structures on the seafloor. Figure 12 B exemplifies this, featuring a Cusk besides an artificial object on the seafloor. Atlantic hagfish was only observed in area B with a widespread distribution, as pictured in Figure 18 A. Registered specimen of Blackmouth catshark, Angler, Rock grenadier and Pleuronectidae ranged between 1 and 8 individuals in the two areas (see Table 4 for details).

When merging the photomosaic sequences, the scope of possible re-counting became visible (Figure 19), as an impact of the overlaying procedure. The scope of re-counting as well as issues related to registration of motile OOI will be thoroughly highlighted in the Discussion section.

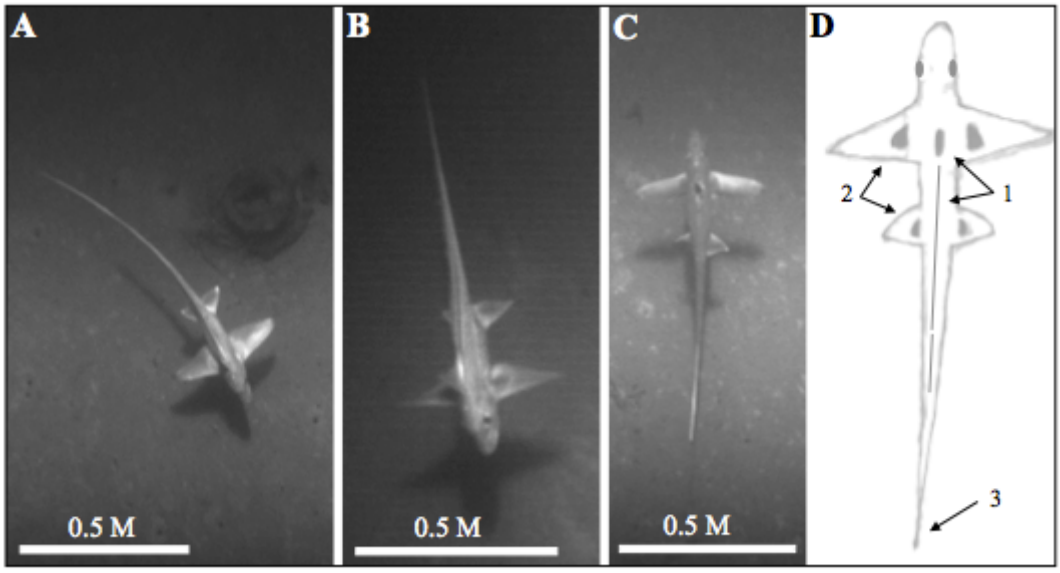

Figure 13. Photos of Rabbit fish (*Chimaera monstrosa*) taken by monochromatic photomosaic camera (A – C). Schematic drawing (D) illustrates characteristics seen from a "bird's-eye view". The first dorsal fin is short and pointed and the second dorsal fin is long and low (1). 2 indicates pectoral and pelvic fins with dark areas at the basis due to thick tissue (depends on viewing angel), while 3 indicates a long, pointed tail (Muus and Nielsen, 2012).

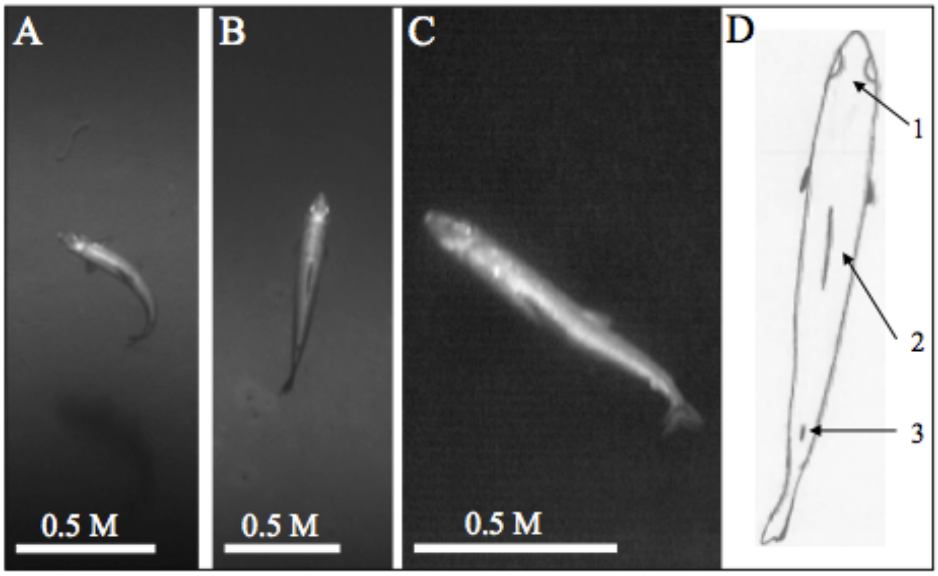

Figure 14. Photos of individuals of Herring smelt family (Argentinidae spp.) taken by monochromatic photomosaic camera (A – C). D displays a schematic drawing from a "bird's-eye view". Characteristics: Individuals observed with a light spot on the back head (1), a single dorsal fin (2) and an adipose fin (3). C) Shows that the anal fin starts where the dorsal fin ends, a characteristic that was possible to see for some individuals captured from the side.

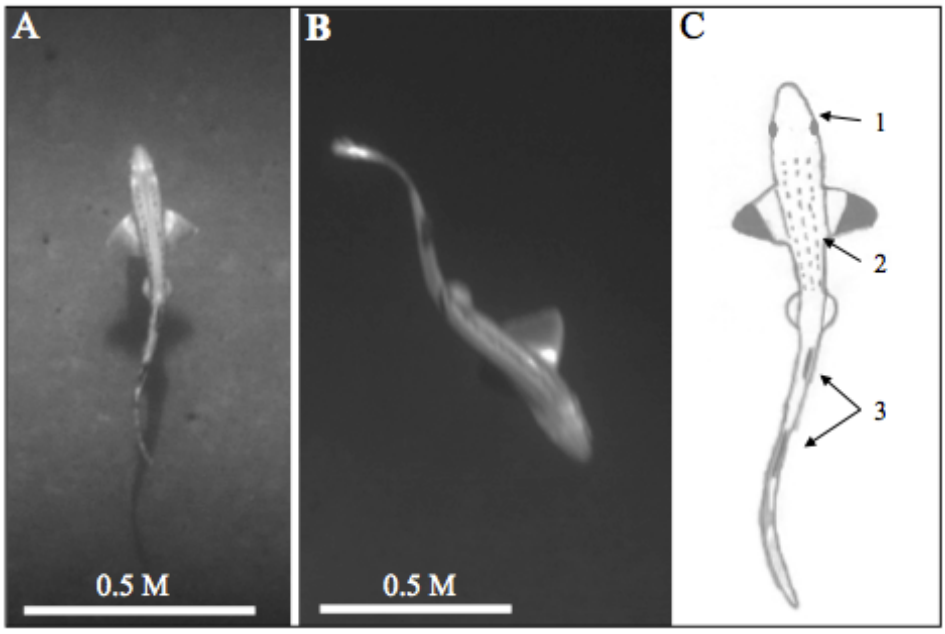

Figure 15. Photos of Blackmouth catshark (*Galeus melastomus*) captured by the photomosaic camera (A and B). C displays a schematic drawing from a "bird's-eye view". Characteristics: The snout is longer than wide (1), body with circular drawings (2), two dorsal fins (3) (Muus and Nielsen, 2012).

Table 4. Number of individuals (ind.) captured by photomosaic camera identified to order and/or family and species in area A and B.

Order	Family	Species	Ind. in area A (31 476 m^2)*[1]	Ind. in area B (7763 m^2)*[2]
Fish				
Gadiformes	Lotidae	Cusk (*Brosme Brosme)*	8	4
Chimaeriformes	Chimaeridae	Rabbit fish (*Chimaera monstrosa*)	80	35
Argentiniformes	Argentinidae (Herring smelts)	Greater argentine (*Argentina silus*)/ Lesser argentine (*Argentina sphyraena*)	49	101
Carcharhiniformes	Scyliorhinidae	Blackmouth catshark (*Galeus melastomus*)	5	2
Myxiniformes	Myxinidae	Atlantic hagfish (*Myxine glutinosa*)		25
Lophiliformes	Lophiidae	Angler (*Lophius piscatorius*)	1	
Gadiformes	Macrouridae	Rock grenadier (*Coryphaenoides rupestris*)	1	1
Pleuronectiformes	Pleuronectidae (Righteye flounders)		1	5
Echinoderms				
Forcipulatda (Sea stars)			8	4
Actinidaria				
Actiniaria*[3] **(**Sea anemones)			485/90	24/54
Crustaceans				
Decapoda (Crabs)	Geryonidae/ Cancridae		61	6

*[1] Counted area (Including overlap). Ground area (Excluding overlap) is 25 414 m^2.

*[2] Counted area (Including overlap). Ground area (Excluding overlap) is 6379 m^2.

*[3] Hard/soft substrate.

Table 5. Fish and benthos abundance in area A and B based on photomosaic images.

Order	Family	Species	Abundance area A (per/1000 m^2)*[1]	Abundance area B (per/1000 m^2)*[1]
Fish				
Gadiformes	Lotidae	Cusk (*Brosme Brosme)*	0.25	0.51
Chimaeriformes	Chimaeridae	Rabbit fish (*Chimaera monstrosa*)	2.54	4.51
Argentiniformes	Argentinidae (Herring smelts)	Greater argentine (*Argentina silus*)/ Lesser argentine (*Argentina sphyraena*)	1.56	13.01
Carcharhiniformes	Scyliorhinidae	Blackmouth catshark (*Galeus melastomus*)	0.16	0.26
Myxiniformes	Myxinidae	Atlantic hagfish (*Myxine glutinosa*)		3.22
Lophiliformes	Lophiidae	Angler (*Lophius piscatorius*)	0.03	
Gadiformes	Macrouridae	Rock grenadier (*Coryphaenoides rupestris*)	0.03	0.13
Pleuronectiformes	Pleuronectidae (Righteye flounders)		0.03	0.64
Echinoderms				
Forcipulatda (Sea stars)			0.25	0.52
Actinidaria				
Actiniaria*[2] **(**Sea anemones)			15.41/2.86	3.09/6.96
Crustaceans				
Decapoda (Crabs)	Geryonidae/ Cancridae		1.94	0.77

*[1] Based on counted area.

*[2] Hard/soft substrate.

4.4 Image quality obtained from Reflection and ArcMap

The screening of the images was done in Reflection, while the mosaic sequences were put in a spatial context in ArcMap. The difference in image quality is expressed in Figure 16-18 to illustrate the loss of spatial resolution in the process. Figure 16 D (upper panel) shows the presence of duplication (here for a Blackmouth catshark) as the images are spatially aligned in ArcMap enabling structures to re-occur to a larger extent to what would be expected. Due to geo-localisation of each

pixel, the sequences are obtained in a different, more correct way in ArcMap compared to Reflection where the pixels are presented in a non-spatial context. When obtained in ArcMap, each single image has a more stretched appearance than observed in Reflection.

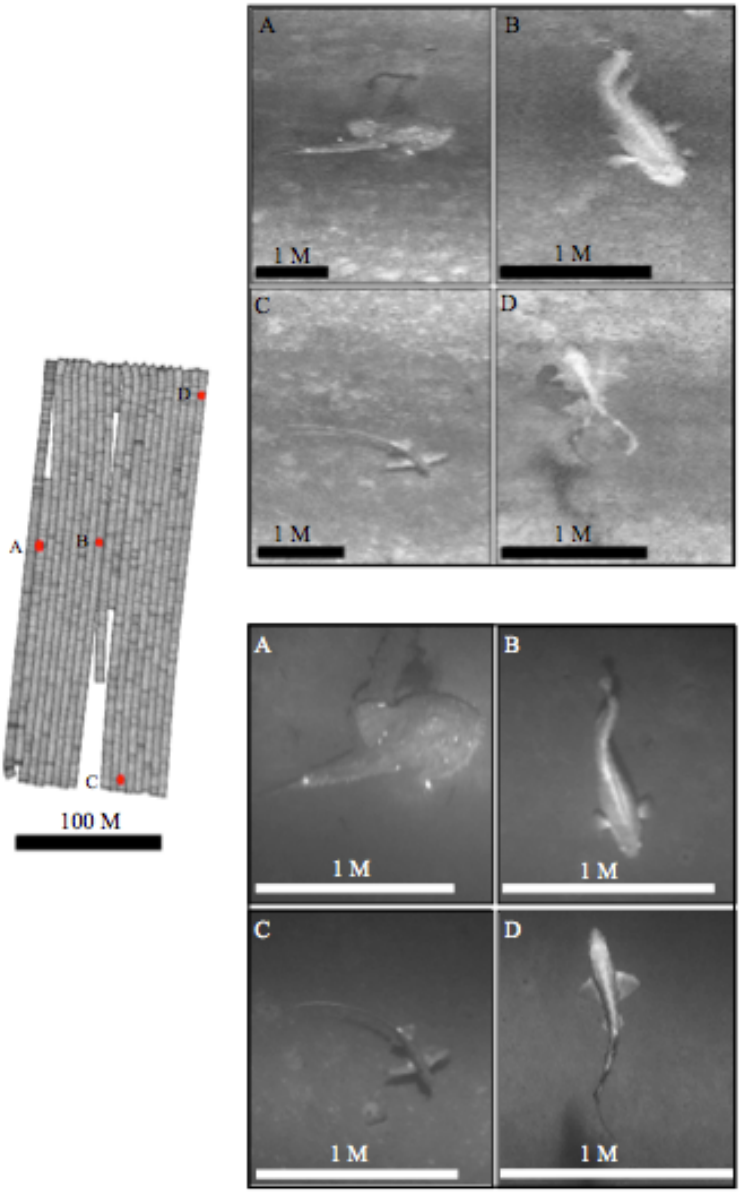

Figure 16. Observed fish in area A with ArcMap images of photomosaic images of low spatial resolution (upper panel, A-D) and corresponding images exported directly from Reflection with high spatial resolution (lower panel, A-D). Figure to the left indicates where the species were found in area A. A) denote Angler, B) Cusk, C) Rabbit fish and D) Blackmouth catshark.

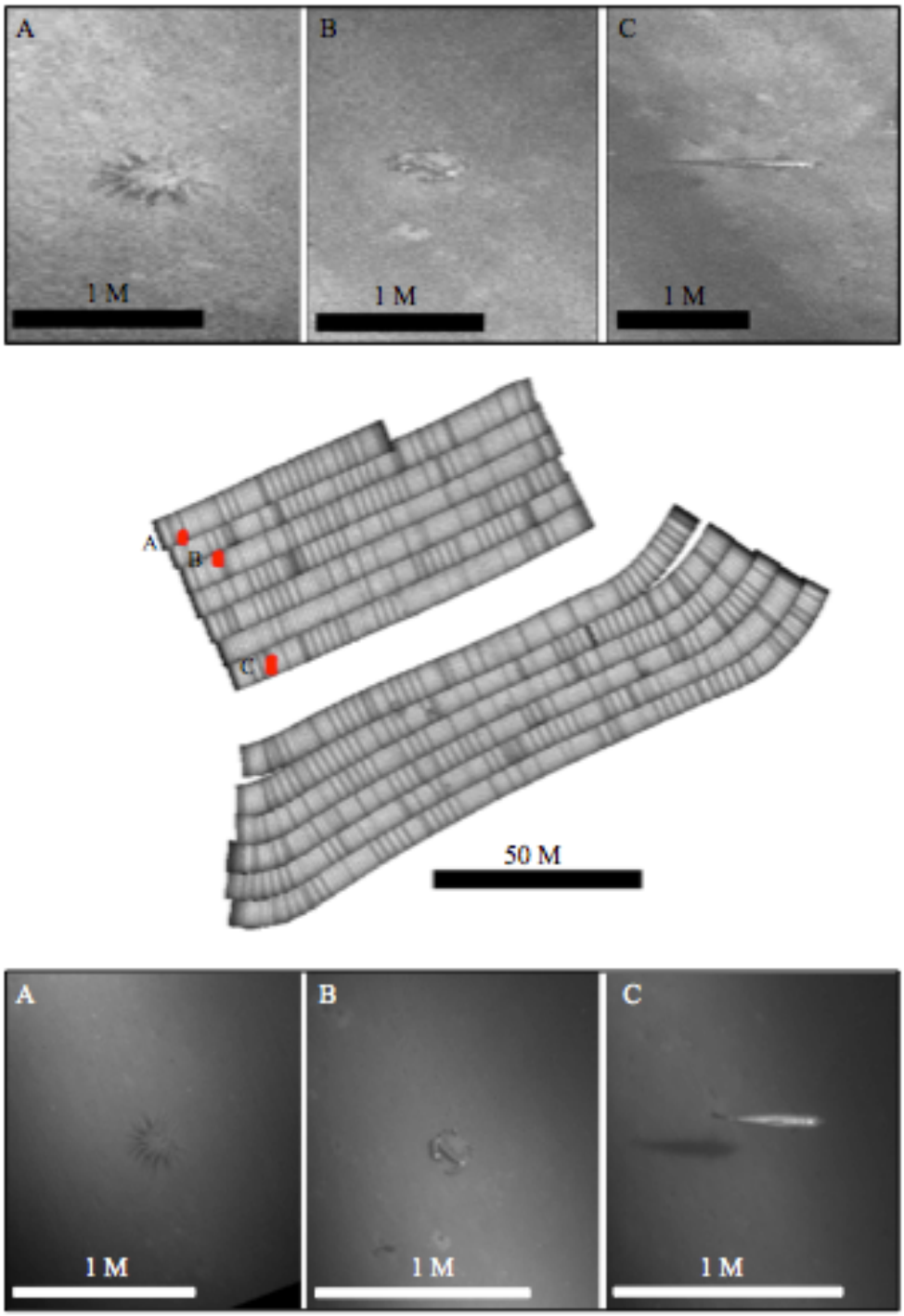

Figure 17. A selection of observed species in area B. Photomosaic images obtained from ArcMap (Upper panel, A-C) and corresponding images seen in Reflection (Lowe panel, A-C). A) denote sea anemone, B) Cancridae spp. and C) Herring smelt.

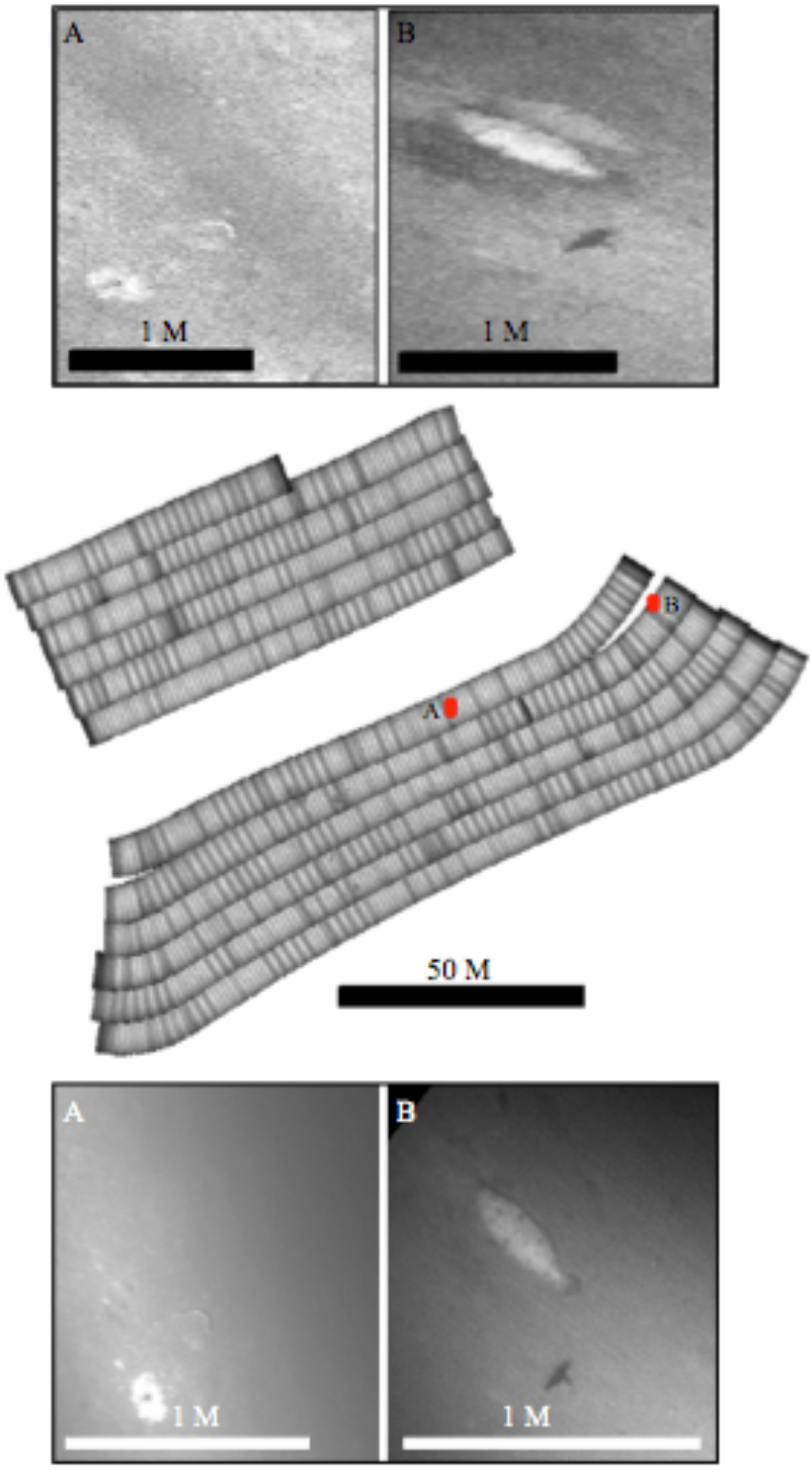

Figure 18. Atlantic hagfish and a Righteye flounder observed in area B. Photomosaic images seen in ArcMap (Upper panel, A and B) and corresponding images obtained in Reflection (Lowe panel, A and B). A) denote Atlantic hagfish and B) Pleuronectidae spp.

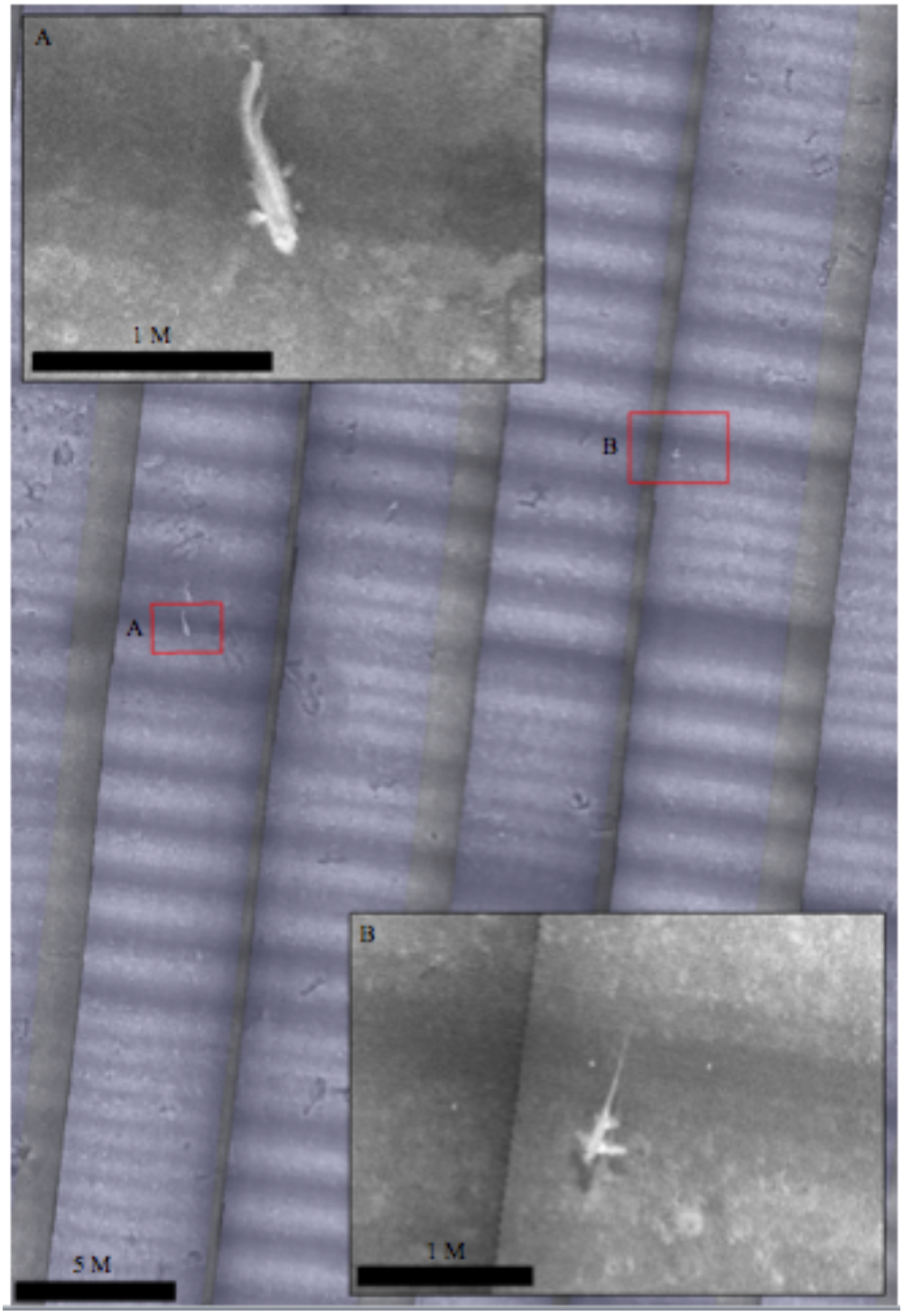

Figure 19. Photomosaic from area A with inset maps showing a Cusk (A) and a Rabbit fish (B) placed in a spatial context. The photomosaic sequences are presented with 30% transparency to illustrate overlaying of images taken from different transect lines.

5 Discussion

The presented work is, to my knowledge, the most extensive survey aimed at mapping benthic organisms at 600 m depth covering 39 200 m^2 using AUV equipped photomosaic camera and HISAS. HISAS provides large areal coverage with low spatial resolution over the dumping site for an overview of OOI. For detailed information on biology, the photomosaic camera provides imagery of high spatial resolution and lower spatial coverage. Rabbit fish and Herring smelts were the most abundant fish species in area A and B, respectively, while numerous specimens of sea stars, sea anemones and crabs were identified to lowest identifiable taxa. An evaluation of the different techniques by means of identification and mapping of OOI, spatial distribution of fish, HUGIN 1000 as survey tool and possible future perspectives will be elaborated in the following sections.

5.1 Identification and mapping of OOI by means of HISAS imagery covering 39 200 m^2 of seafloor

HISAS images covering the same area as the photomosaic imagery (39 200 m^2) were selected for screening of OOI (area A and B in Figure 8). This was done due to the ability to compare similar structures from the images (acoustic and optical) and the presence of interesting OOI such as aggregations of fish revealed by the photomosaic imagery.

The HISAS imagery includes bathymetry providing additional information about seafloor structure in relation to biology. Since the study area consists of soft bottom, the strongest signals (obtained as white structures) are assumed to be solid objects of human made origin; hence HISAS can detect abnormalities that might be related to biology (exemplified by bombes in Figure 9). Soft-bodied organisms absorb the acoustic waves and will therefore not be visible in the images. Anthropogenic structures might attract organisms by serving as artificial habitats (Zintzen et al. (2006), Watters et al. (2010)). That being said, HISAS is a suitable technique for initial search and mapping (Ludvigsen et al., 2014) rather than at providing detailed biological information.

Objects believed to be fish were observed in the data, but the level of detail made differentiation between fish and other structures difficult. The HISAS imagery relies on time demanding interpretation, but it is to my knowledge, not possible to identify fish to species by using this technique solely (Ekehaug, 2013). Simultaneous collection of HISAS and photomosaic imagery, despite operational differences, might facilitate comparison of moving objects such as schooling fish.

HISAS mounted on an AUV provides large spatial coverage (2.6 km^2/h, operation geometry dependent), but the observed spatial resolution is not adequate for identification and mapping of demersal fish and other benthos. This can be achieved by means of optical images (Tilefish camera).

5.2 Identification and mapping of OOI by means of photomosaic camera imagery covering 39 200 m^2

The optical images from this study has revealed the potential of a photomosaic camera in producing imagery with high spatial resolution (1x1 cm) for the identification of several species of demersal fish and other benthic organisms. All of the counted fish findings were identified to species except for the Pleuronectidae spp., possibly Witch flounder based on observations in area (Johnsen, 2015), due to the established identification protocol (see Results section). Some species of fish (e.g. Rabbit fish and Blackmouth catshark) were more readily identified than others with less distinguishable morphological characteristics. The sea stars and anemones were identified to order, whereas the crabs were identified to family. In the process of identification, I had to reconcile with the lowest identifiable taxa to ensure the reliability in the presented data. It should be noted that the results are applicable for benthos and fish that appeared under the field of view of the Tilefish camera solely (6 – 6.5 m over the seafloor).

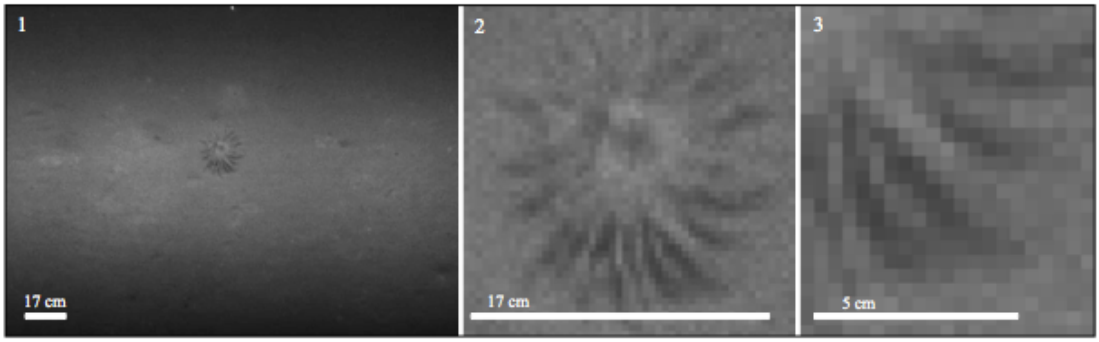

Figure 20. Sea anemone with different magnification and spatial resolution (1-3). In image 3 (and partly 2) single pixels are visible. The figure illustrates how details disappear when magnification increase, making specific identification difficult. Pictures obtained from area B.

Figure 20 and 21 illustrates spatial resolution observed at different magnifications. In images 1 and 2 in both figures it is possible to identify objects to their most accurate taxon level (order or family), but the level of details needed for specific species identification is not possible based on the images. Images 3 (and partly 2) in the figures display imagery of high magnification where single pixels are observed. This might retain information necessary for distinguishing between different species. The crab in Figure 21 is believed to be *Geryon tridens* based on observations in this area (Johnsen, 2015)

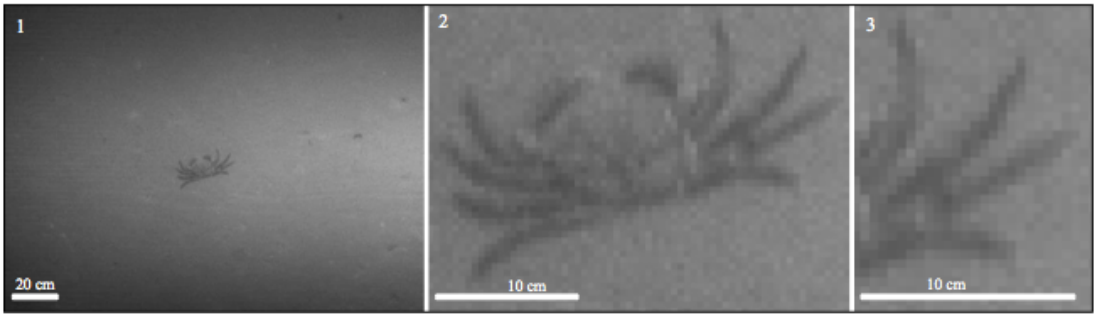

Figure 21. Crab (Geryonidae, possibly *Geryon tridens*) obtained with increased magnification illustrating loss of detail (1-3), respectively. In image 3 (and partly 2) single pixels are visible. Pictures obtained from area B.

When using still images for identification of OOI under present conditions, many challenges arise in terms of understanding what kind of information that is possible to derive from each image (exemplified in Figure 9 (C) and 22). The image quality of single images in the photomosaic was sharpest in the centre, making structures in the

corners more difficult (due to blurring) to identify. This marked a division between less characteristic and morphological distinguishable characteristic OOI. This was also noticeable for OOI outlined by living and human made structures on the seafloor, which made identification even more difficult.

Johnsen et al. (2013) operates with four categories of resolution, whereas two are applicable in this context: 1) spatial resolution (sensor area, image pixel size, pixel density and pixel numbers in a given sensor) and 2) radiometric resolution (bits per pixel, also called dynamic range). Spatial resolution obtained from an image is related to the distance from sensor to the target and the signal-to-noise ratio of the sensor. Singh et al. (2004) mentions the difficulties of identifying benthic organisms to species level with an operational altitude longer than 4 m. This supports the difficulties faces in this thesis where the operational altitude was 6 – 6.5 m.

Radiometric resolution signifies how many digital levels that determine the radiometric precision of a measurement with over exposure (white image) and under exposure (dark image) as the extremes denoting the dynamic range between dark and white, i.e. different grey tones. The photomosaic camera used in this survey operates with a bit rate of 12 enabling sampling of a dynamic range of 4096 intensities of grey tones per image pixel. A large dynamic range is particular important in the process of identifying OOI appearing as different grey tones in this study ((Illunis LLC), Johnsen et al. (2013)).

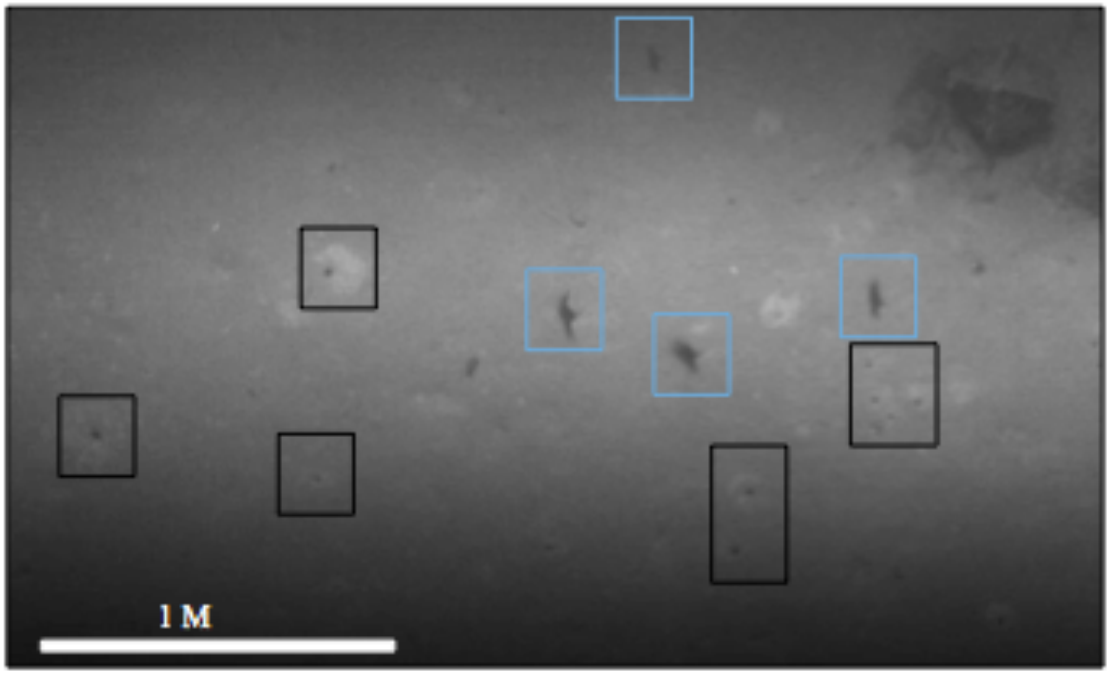

Figure 22. Image of seafloor with dark circular spots believed to be breathing holes (bioturbidity) of organisms buried in the sediments (black squares) and structures of unknown origin (blue squares) that appeared throughout the entire dataset. Picture obtained from area B.

The time span for the screening (overall screening of the photomosaic area) and systematizing of the images (Figure 11) was approximately 12 days (8 hours per day). During that period the entire dataset was screened once, while uncertainties (in terms of identification) were noted and gone through thoroughly afterwards (30 days). Many potential OOI had to be excluded due to low spatial resolution obtained in the imagery as well as fast moving OOI (fish) in the fringe of the images. Reconciling with this fact took time, as I wanted to identify as many OOI as possible.

I noticed a difference from start to end of the identification process in terms of enhanced level of species identification skill that might have affected the results. However, by doing a pilot project like this, many sources of error are present and appear during the identification process. I had to rely on the identification criteria stated; hence, the results represent a conservative estimate of the species diversity, abundance and richness present in the survey area.

5.3 Spatial distribution of fish

The mapping survey represents images in a "bird's-eye view" making identification and quantification of biological OOIs challenging. For fish identification, most characteristics are solely based on identification in a side view. Because of this, a new identification protocol (criteria) had to be established in this study, to ensure proper identification (exemplified in Figure 12 – 15). In the following section, the major findings related to spatial distribution of the fish species (including number of individuals counted) will be elaborated. It should be stated that the following discussion is based on photomosaic imagery.

Figure 11 displays the spatial distribution of fish and gives a view of the variation in species density as well as fish species identified in the study area. The difference in numbers of observed individuals of each species also provides information on abundance (Table 5).

As seen in Table 6 the coefficient of variation (CV) ranges from 35 – 40 % for the photomosaic sequences of similar length (transect lines) from area A and B, respectively. This can be interpreted as an indication of patchiness of fish distribution (See figure 11 for visualization). According to quality requirements related to mapping listed in European standard (European Committee for standardization, 2012), still images covering an area of 0.25 – 2 m^2 for each 30^{th} m is sufficient for mapping. In this survey, still images (each image area of approximately 6 m^2, compiled in a photomosaic) covering the entire seafloor within the survey area were used. This enables larger coverage and visualization by means of maps, providing a better statistical background. The calculations in Table 6 are based on overall fish counting in area A (16 photomosaic sequences of circa 1740 m^2 and 270 m transect length) and B (6 photomosaic sequences of circa 480 m^2 and 77 m transect length), respectively (visualized in Figure 23). Area B is listed with the highest percentage CV as can be related to the patchiness of fish observed for in some transect lines in area B in Figure 23.

Table 6. Statistics indicate mean number of fish specimens (mean), the corresponding standard deviation (SE) and coefficient of variation of mean value in ± % (CV ± %). The statistics are based on based on 16 photomosaic sequences (transect lines) of similar areal coverage and length from area A and 6 photomosaic sequences of similar areal coverage and length from area B.

Area	Mean	SE	CV ± %
A	7.9	2.8	35
B	10.3	4.1	40

The presence of Herring smelts in area B was highlighted in the Result section and did constitute a numerous contribution to the overall number of fish counted in that area. Herring smelts are known to live in schools (Muus and Nielsen, 2012), but they were rather observed to appear in low density numbers in area A and with relatively high density numbers in area B. This difference might be due to the observed difference in bottom structure between the areas.

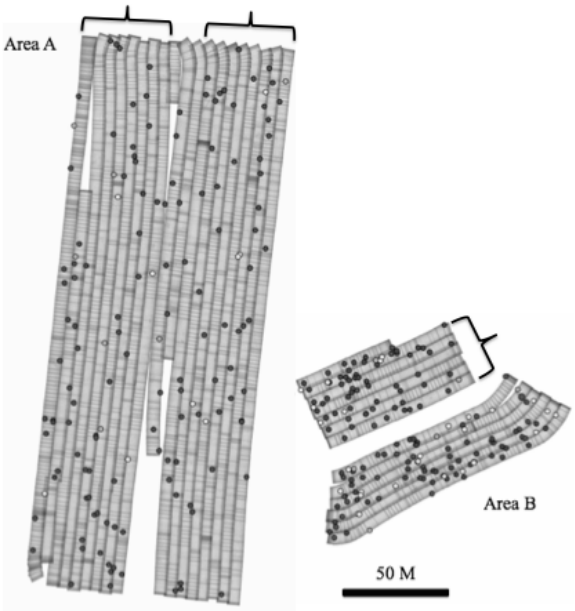

Figure 23. Study area A and B with overall distribution of fish findings (patchiness) marked with greyscale spots. Transect lines used for determination of CV labelled with black curly brackets.

Observed individuals of Rabbit fish displayed a wide spread consistent distribution throughout area A and B, with 80 and 35 observed individuals, respectively. It is known to be an abundant fish among the Chondrichthyans in the northern areas of the Norwegian coast (Williams et al., 2008) and had the highest abundance among all fish species registered in area A and the second highest abundance in area B.

Individuals of Cusk tended to appear in close approximation (around and within) to hard structures on the seafloor (Figure 12 (B) and 24) with a spread distribution. According to a survey conducted by Costello et al. (2005) Cusk might inhabit both cold-water coral reef and soft bottom habitats, as I have observed in ROV footage from coral reefs in Trondheimsfjorden. The survey area might possess intermediate habitat conditions with presence of hard structures on soft bottom, that could support the area with species (prey) not associated with the area originally (Watters et al. (2010)).

Atlantic hagfish was only observed in area B and with a wide spread distribution (Figure 11). Findings might be explained by the fact that the relatively homogenous seafloor in that area made it easier to spot individuals.

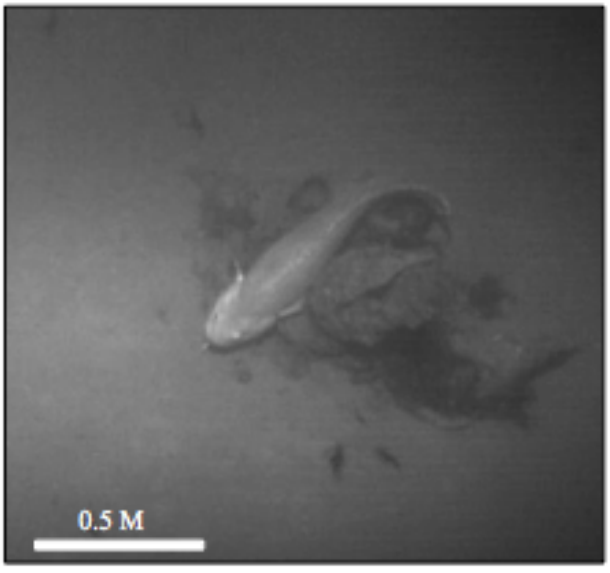

Figure 24. Cusk was frequently observed among and/or within anthropogenic structures on the seafloor. The image shows a Cusk besides what is believed to be the rear end of a bomb. Picture obtained from area B.

For other fish findings (Blackmouth catshark, Angler, Rock grenadier and Pleuronectidae spp.), the numbers of individuals were low with an observed random distribution, making interpretation of fish distribution difficult.

Table 7. Fish abundance (numbers of individuals) as total for area A and B of 1000 m^2 (See Table 5 for abundance of each registered fish taxa).

Area	Total fish abundance (numbers, per 1000 m^2)
A	9.2
B	22.28

5.4 Re-counting of fish (moving OOI)

The occurrence of re-counting is presumably present in the results, but quantifying the extent is difficult due to several reasons. Overlaying photomosaic sequences (Figure 25) constitutes 19.15 and 17.75 % for area A and B, respectively, despite the fact that a lot of the data were excluded based on this issue. The counted species differs in mobility (e.g. non-moving sea anemones, slow moving crabs and fast moving fish). Hence, it is plausible to assume that re-counting may be more evident on fast swimming OOI than non-mobile benthos. Some re-counting might occur due to overlaying created by merging of the mosaic while other might be explained by organisms (fish) moving throughout the study area when surveyed. One can neither deny nor confirm if an individual is registered more than once when the screening of the imagery in Reflection under the circumstances of this thesis. This plausible movement pattern is attempted illustrated for Rabbit fish in the inset map in Figure 25. Re-occurrence of the same OOI obtained in the merged photomosaic can also be seen in the inset map in Figure 25 (blue square). This, together with specimen moving in the same direction as the AUV (hence, appearing in several images), was taken into account when working in Reflection. This supports the importance of identification of OOI in Reflection contra ArcMap, where the imagery appears different.

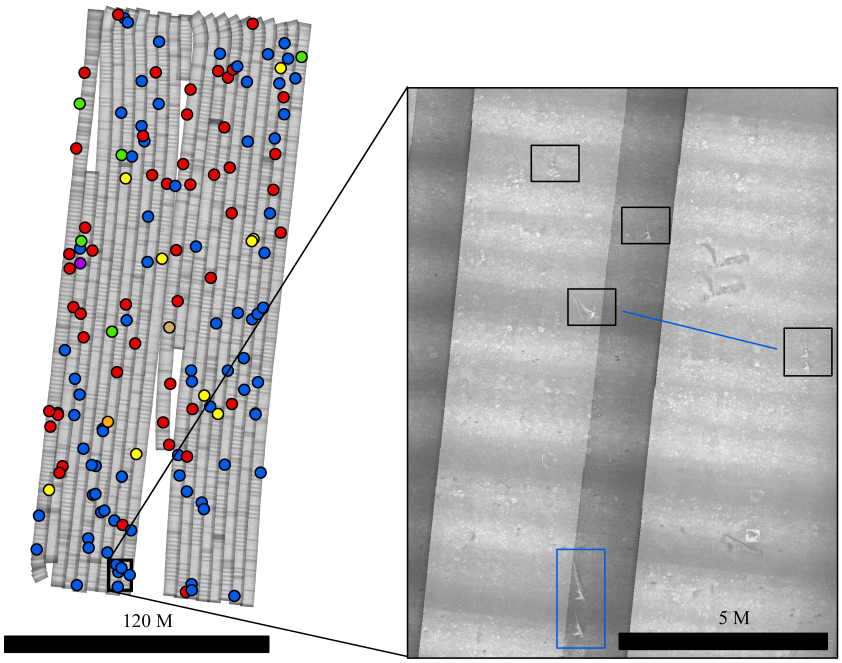

Figure 25. Area A with coloured labels representing fish species found. Inset map (right): Dark grey lines indicates the extent of overlaying present when merging photomosaic sequences (30 % transparency applied), squares shows individuals of Rabbit fish, whereas the blue square highlights the re-occurrence of the same specimen. Blue line illustrates a possible movement pattern between two of the outlined squares and from one sequence to another.

Avoidance by fish is an important issue independent of sampling method, which has to be taken into account (Tolimieri et al., 2008). A possible approach, as suggested by Tolimieri et al. (2008), is to use a side – or forward – looking camera to enhance species identification using AUV. That being said, I presume that increasing the reliability in the registration (hence image quality) of species appearing in the imagery is an as important issue to cope with.

5.5 HUGIN 1000 as survey tool

The HUGIN 1000 AUV has multiple features that make it attractive as survey platform for identification, mapping and monitoring of biological OOI. Each image pixel in the acoustic and optical imager used in this thesis is geo-localised, which enables re-visiting the same area and creation of time series for monitoring possible changes over time. The primarily application of the HUGIN 1000 AUV include military detection and classification of mines (Hagen et al., 2003); however, the science community has adopted the technology (to their respective field) in the recent years (e.g. Ekehaug (2013), Johnsen et al. (2013), Odegard et al. (2013), Ludvigsen et al. (2014), Denny et al. (2015), Ludvigsen et al. (2015)). The high operational endurance (18-24 hours) and low charge time (5 hours) allows for efficient mapping of features of interest. This, together with a relatively high payload capacity enables high spatial coverage (HISAS) and high spatial resolution (Tilefish camera), makes the HUGIN 1000 a preferable platform for a wide range of operations.

Since AUVs operate different sensors simultaneously, also states one of their advantages. However, the different sensors tend to operate best at different altitudes, speeds etc., as seen in this project. Hence, one has to take into account the trade-off between the operational mission parameters. Knowledge and experience is crucial in the planning and execution of missions involving multiple sensors (Hagen et al., 2008b).

5.6 Future perspectives

In summary, the AUV has proven to be a valuable platform for identification, mapping and for future monitoring (time series) of demersal fish and benthos. Constant use and development of underwater vehicles with instruments aiming at sea exploration (Moline et al. (2005), Johnsen et al. (2013), Ludvigsen et al. (2014)) will without a doubt continue.

One of the developments in automated data gathering involves establishing seafloor based docking stations where AUVs can dock, recharge battery, download data and get new mission plans. This will increase the autonomy of the vehicle, as successfully

tested by e.g. Hobson et al. (2007), and hence contribute to a less time consuming, more automated data gathering with large areal coverage. To facilitate automated identification of OOI, emerging imaging techniques like underwater hyperspectral imager (UHI) should be mounted on AUVs. This can facilitate distinguishing between different OOI on the seafloor based on their inherent optical fingerprints by establishing a spectral library (Johnsen et al., 2013).

Future work should include re-visiting the surveyed site to enable creation of time series to monitor possible changes. Thus evaluating changes in terms of species diversity, abundance and richness. This would provide valuable data for future nature management and decision-making. An interesting approach would be aiming at comparing how different human made structures suites as artificial habitats under conditions present in this survey.

By conducting collaboration surveys one can, by means of different instrument carrying platforms (enable different spatial coverage and resolution), provide cross-disciplinary knowledge of common interest (Ludvigsen et al. (2014), Macpherson et al. (2014), Ludvigsen et al. (2015)). This provides an excellent opportunity for branches of science that might be interested in data that are difficult to obtain alone given economical and practical reasons (Manley (2003), Ludvigsen et al. (2014)). The work conducted in this thesis is an example of such practice.

6 Conclusions

- It is possible to identify hard structures as bombs, but not specimens of demersal fish or benthos with HISAS. The spatial resolution (>5x5 cm) is not sufficient for identification of biological OOI alone, it relies on an optical imager providing a higher level of detail to ground truth findings. Soft-bodied organisms absorb the acoustic signals and affect the detectability of biological OOI in a soft bottom community. Obtained solid structures are believed to be of human origin and can attract organisms by acting as artificial habitats. HISAS provides imagery with co-registered bathymetry of high spatial coverage, suiting as an initial tool in detection of OOI.

- Demersal fish were identified to species level and other benthos to family or order with the photomosaic camera. The spatial resolution (1x1 cm) provides detailed imagery and enable mapping of overall fish findings covering 39 200 m^2 seafloor. This gives a new view on the distribution of different demersal fish species, which might provide better estimates on fish abundance and patchiness. It is not possible to distinguish between single benthic specimens clustered on the seafloor under present conditions. Screening of biological OOI in photomosaic imagery is a time demanding process, taking approximately 8 hours to identify specimens in an area of 6300 m^2. For future counting, a more automated approach would be less time consuming, but dependent on level of experience and skill.

- The HISAS AUV is an efficient and adaptable survey platform for measuring biological OOI by means of optical and acoustic imaging. The next step would include the application of emerging technology for a more automated detection and identification of biological OOI for future nature resource management and decision-making.

7 References

7.1 Literature

AUR-LAB & FFI 2013. Cruise report AUR-Lab & FFI cruise December 2013.

BARRETT, N., SEILER, J., ANDERSON, T., WILLIAMS, S., NICHOL, S. & HILL, S. N. Autonomous underwater vehicle (AUV) for mapping marine biodiversity in coastal and shelf waters: implications for marine management. OCEANS 2010 IEEE-Sydney, 2010. IEEE, 1-6.

BEKKBY, T. R., ELI;ERIKSTAD, LARS;BAKKESTUEN, VEGAR 2009. Spatial predictive distribution modelling of the kelp species Laminaria hyperborea. *ICES Journal of Marine Science: Journal du Conseil,* 66 (10)**,** 2106-2115.

BERGE, J., BÅTNES, A. S., JOHNSEN, G., BLACKWELL, S. & MOLINE, M. A. 2012. Bioluminescence in the high Arctic during the polar night. *Marine biology,* 159**,** 231-237.

BUHL-MORTENSEN, L., HODNESDAL, H. & THORSNES, T. 2010. *Til bunns i barentshavet og havområdene utenfor Lofoten - ny kunnskap fra MAREANO for økosystembasert forvaltning*, Norges geologiske undersøkelse 2010.

CLARKE, M. E., TOLIMIERI, N. & SINGH, H. 2009. Using the Seabed AUV to assess populations of groundfish in untrawlable areas. *The future of fisheries science in North America.* Springer.

CLARKE, M. E., WHITMIRE, C., FRUH, E., ANDERSON, J., TAYLOR, J., ROONEY, J., FERGUSON, S. & SINGH, H. Developing the SeaBED AUV as a tool for conducting routine surveys of fish and their habitat in the Pacific. Proceedings of, 2010.

COSTELLO, M. J., MCCREA, M., FREIWALD, A., LUNDÄLV, T., JONSSON, L., BETT, B. J., VAN WEERING, T. C., DE HAAS, H., ROBERTS, J. M. & ALLEN, D. 2005. Role of cold-water Lophelia pertusa coral reefs as fish habitat in the NE Atlantic. *Cold-water corals and ecosystems.* Springer.

DELANEY, J., HEATH, G. R., CHAVE, A., KIRKHAM, H., HOWE, B., WILCOCK, W., BEAUCHAMP, P. & MAFFEI, A. Neptune: real-time, long-term ocean and earth studies at the scale of a tectonic plate. OCEANS, 2001. MTS/IEEE Conference and Exhibition, 2001. IEEE, 1366-1373.

DENNY, A. R., SÆBØ, T. O., HANSEN, R. E. & PEDERSEN, R. B. 2015. THE USE OF SYNTHETIC APERTURE SONAR TO SURVEY SEAFLOOR MASSIVE SULFIDE DEPOSITS. *Journal of Ocean Technology,* 10**,** 36-53.

DICKEY, T. D., ITSWEIRE, E. C., MOLINE, M. A. & PERRY, M. J. 2008. Introduction to the Limnology and Oceanography Special Issue on Autonomous and Lagrangian Platforms and Sensors (ALPS). *Limnology and Oceanography,* 53**,** 2057-2061.

DOLAN, M. F., BUHL-MORTENSEN, P., THORSNES, T., BUHL-MORTENSEN, L., BELLEC, V. K. & BØE, R. 2009. Developing seabed nature-type maps offshore Norway: initial results from the MAREANO programme. *Norwegian Journal of Geology,* 89**,** 17-28.

EKEHAUG, S. 2013. *The use of Side Scan and Synthetic Aperture Sonar mounted on Autonomous Underwater Vehicles for biological habitat mapping.* MSc, Norwegian University of Science and Technology (NTNU).

EUROPEAN COMMITTEE FOR STANDARDIZATION 2012. European standard. *Water quality - Visual seabed surveys using remotely operated and/or towed observation gear for collection of environmental data.* Brussels.

FERRINI, V. L. & SINGH, H. 2006. FISH_ROCK: a tool for identifying and counting benthic organisms in bottom photographs. DTIC Document.

FOSSUM, T. G., SÆBØ, T. O., LANGLI, B., CALLOW, H. & HANSEN, R. E. HISAS 1030–high resolution interferometric synthetic aperture sonar. Proceedings of the Canadian Hydrographic Conference and National Surveyors Conference 2008, 2008. 1-11.

GAFUROV, S. A. & KLOCHKOV, E. V. 2015. Autonomous Unmanned Underwater Vehicles Development Tendencies. *Procedia Engineering,* 106**,** 141-148.

GOLDBERG, E. D. 1995. Emerging problems in the coastal zone for the twenty-first century. *Marine Pollution Bulletin,* 31**,** 152-158.

GRASSLE, J. F., SANDERS, H. L., HESSLER, R. R., ROWE, G. T. & MCLELLAN, T. 1975. Pattern and zonation: a study of the bathyal megafauna using the research submersible Alvin. *Deep Sea Research and Oceanographic Abstracts,* 22**,** 457-481.

HAGEN, P. E., FOSSUM, T. G. & HANSEN, R. E. Applications of AUVs with SAS. OCEANS 2008, 15-18 Sept. 2008a. 1-4.

HAGEN, P. E., STØRKERSEN, N., MARTHINSEN, B.-E., STEN, G. & VESTGÅRD, K. 2008b. Rapid environmental assessment with autonomous underwater vehicles—Examples from HUGIN operations. *Journal of Marine Systems,* 69**,** 137-145.

HAGEN, P. E., STORKERSEN, N., VESTGARD, K. & KARTVEDT, P. The HUGIN 1000 autonomous underwater vehicle for military applications. OCEANS 2003. Proceedings, 22-26 Sept. 2003. 1141-1145.

HALPERN, B. S., WALBRIDGE, S., SELKOE, K. A., KAPPEL, C. V., MICHELI, F., D'AGROSA, C., BRUNO, J. F., CASEY, K. S., EBERT, C., FOX, H. E., FUJITA, R., HEINEMANN, D., LENIHAN, H. S., MADIN, E. M. P., PERRY, M. T., SELIG, E. R., SPALDING, M., STENECK, R. & WATSON, R. 2008. A Global Map of Human Impact on Marine Ecosystems. *Science,* 319**,** 948-952.

HARRIS, P. T. & BAKER, E. K. 2012. Why Map Benthic Habitats? *In:* BAKER, P. T. H. K. (ed.) *Seafloor Geomorphology as Benthic Habitat.* London: Elsevier.

HOBSON, B. W., MCEWEN, R. S., ERICKSON, J., HOOVER, T., MCBRIDE, L., SHANE, F. & BELLINGHAM, J. G. The Development and Ocean Testing of an AUV Docking Station for a 21" AUV. OCEANS 2007, 2007. IEEE, 1-6.

JOHNSEN, G. 2015. *RE: Benthic communities in Trondheimsfjorden.*

JOHNSEN, G., VOLENT, Z., DIERSSEN, H., PETTERSEN, R., ARDELAN, M. V., SØREIDE, F., FEARNS, P., LUDVIGSEN, M. & MOLINE, M. 2013. Underwater hyperspectral imagery to create biogeochemical maps of seafloor properties. *In:* WATSON, J. & ZIELINSKI, O. (eds.) *Subsea Optics and Imaging.* Woodhead Publishing, 20, 508-540.

LUDVIGSEN, M., JOHNSEN, G., SØRENSEN, A. J., LÅGSTAD, P. A. & ØDEGÅRD, Ø. 2014. Scientific operations combining ROV and AUV in the Trondheim Fjord. *Marine Technology Society Journal,* 48**,** 59-71.

LUDVIGSEN, M., THORSNES, T., HANSEN, R. E., SORENSEN, A. J., JOHNSEN, G., LAGSTAD, P. A., ODEGARD, O., CANDELORO, M.,

NORNES, S. M. & MALMQUIST, C. Underwater vehicles for environmental management in coastal areas. OCEANS 2015-Genova, 2015. IEEE, 1-6.
MACPHERSON, K., KING, P., WALKER, D., LEWIS, R., DEVILLERS, R., MUNROE, J., KENNEDY, N. & VARDY, A. The development of AUV strategies for multidisciplinary use. Oceans-St. John's, 2014, 2014. IEEE, 1-7.
MANLEY, J. E. Autonomous underwater vehicles for ocean exploration. OCEANS 2003. Proceedings, 2003. IEEE, 327-331.
MCHUGH, R. The potential of synthetic aperture sonar in seafloor imaging. Conference proceedings on CD ROM, 2000. 1-7.
MEYER, K., BERGMANN, M. & SOLTWEDEL, T. 2013. Interannual variation in the epibenthic megafauna at the shallowest station of the HAUSGARTEN observatory (79° N, 6° E). *Biogeosciences,* 10**,** 3479-3492.
MOEN, F. E. & SVENSEN, E. 2004. *Dyreliv i havet, nordeuropeisk marin fauna*, KOM Forlag, 1-608.
MOLINE, M. A., BLACKWELL, S. M., VON ALT, C., ALLEN, B., AUSTIN, T., CASE, J., FORRESTER, N., GOLDSBOROUGH, R., PURCELL, M. & STOKEY, R. 2005. Remote Environmental Monitoring Units: An Autonomous Vehicle for Characterizing Coastal Environments*. *Journal of Atmospheric and Oceanic Technology,* 22**,** 1797-1808.
MUUS, B. J. & NIELSEN, J. G. 2012. *Våre Saltvannsfisker,* Gyldendal A/S, Danmark, CAPPELEN DAMM AS, 1-339
ODEGARD, O., LUDVIGSEN, M. & LAGSTAD, P. A. Using synthetic aperture sonar in marine archaeological surveys - Some first experiences. OCEANS - Bergen, 2013 MTS/IEEE, 10-14 June 2013 2013. 1-7.
SAKSHAUG, E. & SNELI, J.-A. 2000a. *Trondheimsfjorden,* Trondheim, Tapir forlag, 12-18.
SAKSHAUG, E. & SNELI, J.-A. 2000b. Trondheimsfjorden. Trondheim: Tapir forlag, 65-75
SAKSHAUG, E. & SNELI, J.-A. 2000c. Trondheimsfjorden. Trondheim: Tapir forlag, 133-148.
SHERMAN, A. D. & SMITH JR., K. L. 2009. Deep-sea benthic boundary layer communities and food supply: A long-term monitoring strategy. *Deep Sea Research Part II: Topical Studies in Oceanography,* 56**,** 1754-1762.
SHUMCHENIA, E. J. & KING, J. W. 2010. Comparison of methods for integrating biological and physical data for marine habitat mapping and classification. *Continental Shelf Research,* 30**,** 1717-1729.
SINGH, H., ARMSTRONG, R., GILBES, F., EUSTICE, R., ROMAN, C., PIZARRO, O. & TORRES, J. 2004. Imaging coral I: Imaging coral habitats with the SeaBED AUV. *Subsurface Sensing Technologies and Applications,* 5**,** 25-42.
SINGH, H., ROMAN, C., PIZARRO, O., EUSTICE, R. & CAN, A. 2007. Towards high-resolution imaging from underwater vehicles. *The International journal of robotics research,* 26**,** 55-74.
SMITH JR, K. L., KAUFMANN, R. S. & WAKEFIELD, W. W. 1993. Mobile megafaunal activity monitored with a time-lapse camera in the abyssal North Pacific. *Deep-Sea Research Part I,* 40**,** 2307-2324.
STATISTICS NORWAY 2013. Oversikt over geografiske forhold. *Statistisk årbok 2013.* Statistisk sentralbyrå.

TOLIMIERI, N., CLARKE, M. E., SINGH, H. & GOLDFINGER, C. 2008. Evaluating the SeaBED AUV for monitoring groundfish in untrawlable habitat. *Marine habitat mapping technology for Alaska. Alaska Sea Grant College Program, University of Alaska Fairbanks*, 129-141.

VON ALT, C. Autonomous underwater vehicles. Autonomous Underwater Lagrangian Platforms and Sensors Workshop, 2003. 1-5.

WATTERS, D. L., YOKLAVICH, M. M., LOVE, M. S. & SCHROEDER, D. M. 2010. Assessing marine debris in deep seafloor habitats off California. *Marine Pollution Bulletin,* 60**,** 131-138.

WILLIAMS, S., PIZARRO, O., MAHON, I. & JOHNSON-ROBERSON, M. 2009. Simultaneous Localisation and Mapping and Dense Stereoscopic Seafloor Reconstruction Using an AUV. *In:* KHATIB, O., KUMAR, V. & PAPPAS, G. (eds.) *Experimental Robotics.* Springer Berlin Heidelberg, 407-416.

WILLIAMS, T., HELLE, K. & ASCHAN, M. 2008. The distribution of chondrichthyans along the northern coast of Norway. *ICES Journal of Marine Science: Journal du Conseil,* 65**,** 1161-1174.

ZINTZEN, V., MASSIN, C., NORRO, A. & MALLEFET, J. 2006. Epifaunal inventory of two shipwrecks from the Belgian Continental Shelf. *Hydrobiologia,* 555**,** 207-219.

ZINTZEN, V., NORRO, A., MASSIN, C. & MALLEFET, J. 2008. Spatial variability of epifaunal communities from artificial habitat: Shipwrecks in the Southern Bight of the North Sea. *Estuarine, Coastal and Shelf Science,* 76**,** 327-344.

7.2 Web citations

1. GEOMARES PUBLISHING BV. 2012 - 2015. *HUGIN* [Online]. Available: http://www.geo-matching.com/products/id1970-hugin.html [Accessed 24.11 2015].
2. ILLUNIS LLC. *Illunis XMV-11000* [Online]. Available: http://alacron.com/clientuploads/directory/Cameras/ILLUNIS/XMV-11M.pdf [Accessed 01.11 2015].
3. KONGSBERG MARITIME. *Autonomous Underwater Vehicle - AUV The HUGIN Family* [Online]. Available: http://www.km.kongsberg.com/ks/web/nokbg0397.nsf/AllWeb/A6A2CC361D3B9653C1256D71003E97D5/$file/HUGIN_Family_brochure_r2_lr.pdf?OpenElement [Accessed 10.09 2015].
4. SCHJERVEN, S. O. 2009. *The HUGIN 1000 AUV as sensor platform for seafloor mapping* [Online]. Kongsberg Simrad. Available: http://departements.telecom-bretagne.eu/data/iti/seafloor/presentations/Kongsberg_Schjerven_The_HUGIN_1000_AUV.pdf [Accessed 15.11 2015].